UNITED NATIONS
UNIVERSITY
GEOTHERMAL TRAINING PROGRAMME
Orkustofnun, Grensásvegur 9,
IS-108 Reykjavík, Iceland

Reports 2010
Number 26

COMPARISON AND SELECTION OF A STEAM GATHERING SYSTEM IN ULUBELU GEOTHERMAL PROJECT, SUMATERA, INDONESIA

A. Novi Purwono
Pertamina Geothermal Energy
Menara Cakrawala 15th Floor
Jl. MH. Thamrin 9,
Jakarta
INDONESIA
novi.purwono@pgeindonesia.com

ABSTRACT

This study focuses on the conceptual design of geothermal pipelines, especially for steam gathering systems. A tool for calculating a pipeline system was developed which emphasizes the comparison and selection of a pipeline system for transmitting geothermal fluids, with respect to optimal design and costs. Certainly it is related to the behaviour of fluid flow in a pipeline system. The calculation compares three different conceptual systems of geothermal fluid transmission: single-phase flow, two-phase flow and a combination of both systems (hybrid). It also compares fluid transmission using a single pipe and two parallel pipes.

A case study is made of a steam gathering system for the Ulubelu geothermal project 2×55 MW, units 1 and 2, the high-temperature geothermal area under development in Indonesia by PT. Pertamina Geothermal Energy. The results show that the three studied systems give a similar design and costs for this project, but the hybrid system would be most efficient with regard to the characteristics of the existing project site. Generally, a single-pipe transmission is more economical than two parallel pipes. There was an insignificant difference in pipe diameter between the designs.

1. INTRODUCTION

Indonesia is located in Southeast Asia and has many islands and active volcanoes. It has great potential in its geothermal resources. Referring to the data from the Directorate General of Mineral, Coal and Geothermal, the Indonesian Ministry of Energy and Mineral Resources, the total geothermal potential is believed to be about 27 GWe at approximately 257 locations. More than 200 volcanoes are located on the islands of Sumatera, Java, Bali and the other islands of eastern Indonesia and are collectively a part of 'The Pacific Ring of Fire' (Azimudin, 2008). This area has a large concentration of high-temperature geothermal systems. In Indonesia, the important use of geothermal energy is to generate electricity. The geothermal development is supported by the government. The contribution of renewable energy, especially geothermal energy, is expected gradually to increase, to replace oil. The installed capacity at the end of 2009 was about 1,179 MW (4.3% of the geothermal potential).

FIGURE 1: Location of Ulubelu Geothermal Project, Sumatera, Indonesia (Courtesy of Google Maps)

1.1 Development of the Ulubelu geothermal project

The Ulubelu geothermal field is one of many potential high-temperature geothermal prospects in Indonesia, especially in Sumatera, and it is one of the PT. Pertamina Geothermal Energy (PGE) geothermal fields. It is located in Ulubelu, District of Tanggamus, Lampung Province, about 100 km west of Bandar Lampung, the capital city of Lampung Province (Figure 1). The Ulubelu prospect is surrounded by Mount Sula in the east, Mount Rindingan in the north and Mount Tanggamus in the south. Ulubelu is classified as a liquid-dominated reservoir system.

The plan is to develop the Ulubelu field into a 5×55 MW geothermal power plant, and the first development is Ulubelu Project units 1 and 2 (2×55 MW). In this project, PT. Pertamina Geothermal Energy is developing steam gathering systems to supply steam to a power plant that will be built and operated by PT. Perusahaan Listrik Negara (state owned company). The drilling is designed to take place in five clusters. The first drill site, well UBL-01, is located in cluster A, and drilling was started in 2007. The average elevation of the site is about 800 m a.s.l. and the site is surrounded by villages, coffee plantations and some paddy fields. Access roads for each cluster have already been built, which will also be used as pipeline routes from each cluster to the power plant.

Scientific data, both surface and subsurface, obtained from three slim holes drilled in the south and three large diameter wells (UBL-2, UBL-3 and UBL-4) drilled in cluster B in the north, show that the northern block has a higher subsurface temperature than the southern block and has a different type of reservoir. This is in accordance with the pattern of the existing geothermal hydrologic system in which an up-flow zone is estimated to be in the northern zone (Pagaralam-Panindayan, Ulubelu) with the out-flow zone in the south (Waypanas PGE, 2008).

1.2 Study description

1.2.1 General overview

In the early stages of any project, the designers need to make estimates for the design, although it is common that information and data are limited. The estimates are therefore based on calculations made

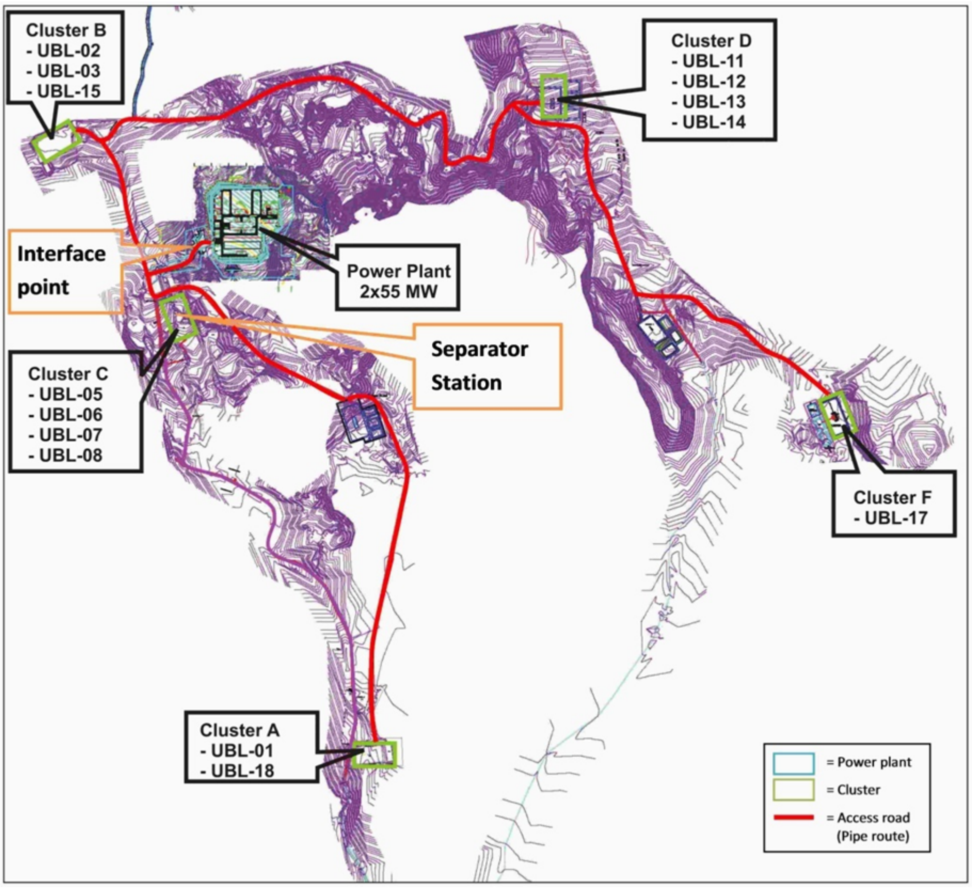

FIGURE 2: Ulubelu field project, units 1 and 2

through a combination of real data, assumptions and rules of thumb that have been widely used in similar projects or cases. These estimations are used to delineate how the project should be executed with reference to optimal design and costs.

This study focuses on the conceptual design and design estimates of a geothermal pipeline for steam gathering systems. It emphasises the comparison and selection of a pipeline design for transmitting geothermal fluids, based on optimal design and costs. The behaviour of fluid flow in pipeline systems is reviewed and pipe diameters, thicknesses and supporting systems are calculated. The calculations compare three different conceptual systems of geothermal fluid transmission: single-phase flow, two-phase flow and a combination of both systems (hybrid).

Figure 2 shows the topographical map of the Ulubelu project. The steam gathering systems will supply steam to the interface point located close to the power plant. Steam will be supplied by eleven production wells located in three clusters, i.e. clusters B, C and D. Brine from the separator and condensate from the power plant will be re-injected into three re-injection wells located in two clusters, i.e. clusters A and F. Brine and condensate are injected into different wells.

In a two-phase flow pipeline, two-phase fluids from wells at every cluster are transmitted to separator stations located in cluster C and all brine from the separator station is re-injected to cluster A. For a single-phase flow pipeline, separators are located in each cluster and steam is transmitted to the power plant. Brine from clusters B and C is re-injected at cluster A, while brine from cluster D will be re-injected at cluster F. The hybrid pipeline scenario is a combination of the other two: two-phase flow from clusters B and C with a separator station located in cluster C, and a steam pipeline from cluster D (individual separator).

Calculations and comparison are also be made between transmission by single pipe and two parallel pipes for each of the pipeline scenarios. Finally, the selection of a pipeline design is based on both the most economical design and its conformity with design criteria with reference to standards and design practices. All calculations are performed with the Engineering Equation Solver (EES) software. Examples of EES calculations are given in Appendix I.

1.2.2 Objectives of the study

The objective of this study is to determine the optimum design of a geothermal fluid flow pipeline for a preliminary design of the project. Calculations include:

a. Mass balance of single-phase, two-phase and hybrid flow pipelines;
b. Pressure drop of single and parallel double pipes for each scenario;
c. Pressure drop in the separator;
d. Pipe thickness;
e. Costs for each scenario; and
f. Length between pipe support and expansion loop design.

The results of these calculations will be compared and the optimum design will be selected. This design selection can be used as a basic design for the project with more detailed calculations. Finally, the calculations can be used as a preliminary design template for other similar projects. The EES program that was developed can be easily rerun as new information becomes available, and the output data will be changed accordingly.

2. BASIC THEORY OF PIPELINE DESIGN

The complete assembly of pipes, including inline components such as pipe fittings and flanges, needs to be considered in the design of steam gathering systems for a geothermal power plant. Pipeline design includes the piping system design and all necessary calculations. Piping systems transmit the fluids that will be used to generate electricity, the main product of a geothermal power plant, and convey the waste fluids to their destinations. Therefore, the efficient operation of the pipelines is an important factor in determining the effectiveness of the entire system. The accuracy and proper selection of piping systems significantly affect the cost of developing a geothermal power plant and/or its supporting facility.

Pipeline design needs to address the interconnections between many variables. Standard design criteria for a pipeline in a geothermal system are described below (Jónsson, 2010):

a. Topology and route selection;
b. Demand and flow analysis;
c. Pipe diameter optimization, related to the minimum total cost with the net present value and the fluid's maximum allowable velocity;
d. Thickness and pressure classes;
e. Mechanical stress analysis of supports, type, and distance between supports;
f. Thermal stress analysis of anchors, expansion loops and expansion units (if any); and
g. Pump size and arrangement.

Design criteria and processes will be different depending on the fluids that are transmitted through the pipeline, whether it is water, steam or two-phase flow. A two-phase flow system will be more complex than a single-phase flow system.

2.1 Topology and route selection

Pipeline route selection plays a major role when designing an effective pipeline system. It also depends on the terrain. The present practice of route selection for geothermal pipelines is governed by factors such as the shortest distance, constructability, minimal effects on the environment, and approachability. The considerations that should be taken into account when designing the pipeline are described below (Jónsson, 2010):

a. The pipeline route shall be chosen as a reasonably short distance between two points, and the number of high and low spots should be minimized. High spots require an avoidance of pressures higher than saturation pressure and low spots require drains; also, the pressure should be checked for the design pressure. In a two-phase flow system, pressure shocks can affect the fluid phase. It can result in a slug flow regime, problems with pipe support, and even ruptured pipes.
b. Routing the pipeline over a moderately sloped terrain makes it easier to install the pipe.
c. There must be access to all portions of the route for piping equipment.
d. Avoid landslide areas and avoid crossing watercourses that are eroding.
e. Avoid crossing federal or state land where possible. Permits are often required for crossing these lands and the permitting process takes a considerable amount of time, cost and effort to complete.
f. The pipeline route should be selected to minimize environmental impacts and visual impact.
g. Full consideration should be given to the possibility of future expansion of the system. If a pipeline extension is anticipated, then pipe size and ratings should be appropriate for the appropriate extension possibilities.

These considerations also depend on whether the pipes are installed underground or above ground. The cost of an above ground pipeline system is less than that for an underground system.

2.2 Cost optimization of pipeline design

One of the main considerations when selecting the optimum pipeline design is to minimize the "Total Updated Cost (C_t)", described below (Jónsson, 2010):

$$C_t = C_c + (C_e\,(1 - 1/(1+i)^T))/i \tag{1}$$

where C_c = Initial cost;
C_e = Annual operational cost;
T = Project expected life time; and
i = Index rate.

The initial cost (C_c) is equal to:

$$C_c = L_p\,k_p + n_b\,k_b + n_c\,k_c + n_u\,k_u + n_v\,k_v + n_d\,k_d + L_p\,k_i \tag{2}$$

where L_p = Pipe length (m);
k_p = Cost of pipe ($/m);
n_b = Number of bends;
k_b = Cost of bends ($/unit);
n_c = Number of connections;
k_c = Cost of connections ($/unit);
n_u = Number of expansion units;
k_u = Cost of expansion units ($/unit);
n_v = Number of valves;

k_v	=	Cost of valves (\$/unit);
n_d	=	Number of pumps;
k_d	=	Cost of pumps (\$/unit); and
k_i	=	Cost of insulation (\$/m).

The annual operational cost (C_e) is equal to:

$$C_e = k_e \, o_h \, P \tag{3}$$

where k_e = Cost of electrical energy (\$/kWh);
o_h = Hours in one year = 365 × 24 = 8760 hours; and
P = Power of the pump (kW).

Because the annual operational cost is related to pumping power, it is only considered when the pipelines transmit water and need to be pumped, such as when the pressure drop of the pipelines is higher than the initial pressure of the system, or where there is no initial pressure in the system.

As mentioned before, the total updated cost (C_t) is the main parameter for selecting the optimum diameter of the pipeline with respect to the maximum allowable velocity of the fluid in the pipeline. The total updated cost of each pipe diameter should be calculated; the minimum total updated cost gives the optimum diameter of the pipeline design. Figure 3 shows an example of the selection of the optimum diameter based on the minimum total updated cost. It is obvious that increasing the diameter of the pipe is responsible for increasing the initial cost of the pipe. But the updated annual operational cost would decrease. The minimum total updated cost indicates the optimum diameter of the pipe.

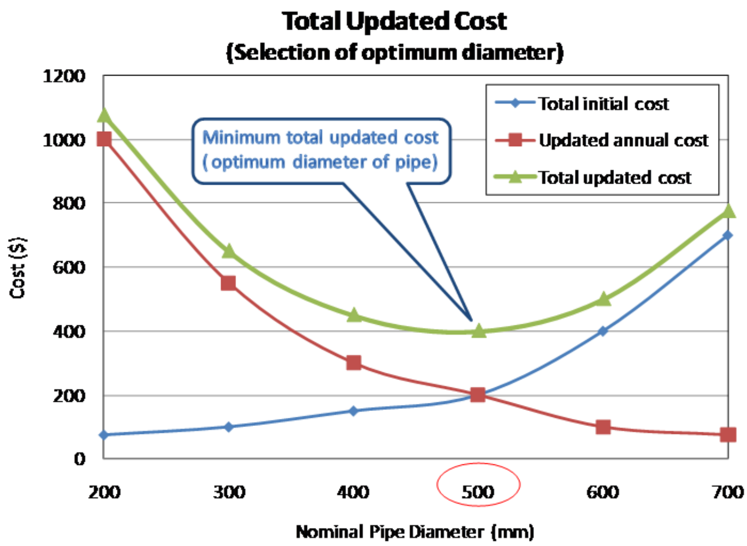

FIGURE 3: Graph of the optimum pipe diameter selection

In this study, for two-phase flow and water without pump (water moved by gravity), the annual operational cost is very low. Hence, the pipe diameter should be selected based on the minimum initial cost and the proper velocity of the fluid in order to avoid corrosion and erosion in the pipeline. The velocity of the water in a pipeline should be less than 3 m/s, and it should be less than 40 m/s for steam. However, when a pipeline transmits either steam or two-phase flow from the wellhead, decreasing the diameter of the pipe leads to an increased pressure drop in the system. This will reduce the capital expenditure for the pipe; on the other hand, it often proves to be uneconomical when total costs are considered. Higher pressure drop means the wellhead must operate with a higher wellhead pressure, and since the flow and pressure in the well will decline with time, it will affect the life supply of the well, requiring a make-up well earlier than would be the case if the pressure drop was lower.

2.3 Single-phase flow fluid transmission

The main factors involved in pipeline design are (Pálsson, 2010):

a. Pressure drop because of flow in the pipeline. In this case, the pipe diameter plays a major part as well as bends, flanges and other irregularities in the pipe layout.

b. Heat losses to the environment. In order to maintain the heat of transmitted fluids, pipes are frequently insulated, as in the case of district heating pipes.
c. Structural strength of the pipeline systems. This involves necessary pipe thickness to withstand pressure as well as other external loads. Loads can be from many sources, such as wind, earthquakes, collision and also if the flow changes suddenly; thus, large forces can be generated.

Designing steam gathering systems for a geothermal power plant always involves single-phase flow through a pipeline. It can be steam or water flow such as brine and condensate from the power plant. Pressure drops that occur in the single-phase flow are due to friction along the pipe and to elevation changes.

2.3.1 Pressure drop due to friction

Pressure drop due to friction (ΔP_f) can be calculated from the friction head (H_f) that is generated in the pipeline system. In order to calculate friction head, first the velocity of the fluid (V) should be calculated, using the following equation (Jónsson, 2010):

$$V = Q / (\pi D_{in}^2 / 4) \tag{4}$$

where V = Average velocity of fluid (m/s); and
D_{in} = Pipe inner diameter (m).

As mentioned before, in order to avoid corrosion and erosion in the pipeline, the velocity of the water in the pipeline should be less than 3 m/s, and less than 40 m/s for the steam velocity. Water velocities should be limited because small rough spots on pipe surfaces can cause local concentrations of friction that could lead to the formation of steam bubbles.

The equivalent length (L_e) can be calculated using Equation 5:

$$L_e = L_p + n_b h_b D_{in} + n_c h_c D_{in} + n_u h_u D_{in} + n_v h_v D_{in} \tag{5}$$

where L_p = Pipe length (m);
D_{in} = Pipe inner diameter (m);
h_b = Equivalent length of bends, 20;
h_c = Equivalent length of connections, 20;
h_u = Equivalent length of expansion units, 20; and
h_v = Equivalent length of valves, 13.

The Reynolds number (Re) should be calculated using Equation 6:

$$Re = \frac{\rho V D_{in}}{\mu} \tag{6}$$

where ρ = Density of fluid (kg/m^3); and
μ = Dynamic viscosity of fluid (kg/ms).

The Reynolds number describes the fundamental characteristics of the flow. Specifically it determines whether the flow is *laminar* or *turbulent.* Laminar flow occurs at low Reynolds numbers, where viscous forces are dominant, and is characterized by smooth, constant fluid motion, while turbulent flow occurs at high Reynolds numbers and is dominated by inertial forces.

Based on the value of the Reynolds number, the friction factor (f) should be calculated from Equation 7 for laminar flow and Equation 8 for turbulent flow. Equation 8 is the *Swamee–Jain* equation used to solve directly for the *Darcy–Weisbach* friction factor f for a full-flowing circular pipe. It is an approximation of the implicit Colebrook–White equation.

$Re \leq 2100$ $$f = 64 / Re \tag{7}$$

$Re > 5000$ $$f = \frac{0.25}{\left(log_{10}\left[\frac{\varepsilon}{3.7D_{in}} + \frac{5.74}{Re^{0.9}}\right]\right)^2} \tag{8}$$

where Re = Reynolds number; and
ε = Absolute roughness of pipe (m).

Friction head (H_f) in m can be calculated by:

$$H_f = \frac{f\, V^2 L_e}{2\, g\, D_{in}} \tag{9}$$

where g = Acceleration due to gravity.

Thus, the pressure drop due to friction can be calculated by:

$$\Delta P_f = \rho\, g\, H_f \tag{10}$$

2.3.2 Pressure drop due to elevation change

The pressure drop due to elevation change (ΔP_H) can be calculated by:

$$\Delta P_H = \rho\, g\, (Z_e - Z_s) \tag{11}$$

where Z_e = Elevation at the end point of pipe (m); and
Z_s = Elevation at the start point of pipe (m).

2.3.3 Total pressure drop of single-phase flow fluid transmission

The total pressure drop of single-phase fluid transmission (ΔP_t) is expressed as:

$$\Delta P_t = \Delta P_f + \Delta P_H \tag{12}$$

In a water pipeline system, a negative ΔP_t indicates that it is not necessary to pump the fluid, as it will flow by gravity.

2.4 Two-phase flow fluid transmission

One method for transmitting fluid through a pipeline is two-phase fluid transmission. This method carries steam and hot water together in the same pipe. Based on experience, the pressure drop that occurs in the two-phase flow is higher than when transmitting steam alone, hence, more attention is needed when determining the design of a two-phase flow pipeline. The claimed advantages of two-phase transmission are as follows (Armstead, 1978):

a. The savings in wellhead gear can outweigh the extra cost of the rather larger pipe work.
b. The adoption of relatively large separators close to the utilization plant has an economic "scale effect" advantage compared to the use of many smaller individual wellhead separators, and their maintenance can be more easily and cheaply handled.

c. Significant amounts of additional power can be extracted from the hot water by multiple flashing at the plant without the use of a costly separate hot water collection and transmission scheme with its attendant controls.
d. The wasteful rejection of hot well water at the wellheads can be avoided, thereby not only conserving energy and reducing heat pollution but also saving costly drainage channels. With two-phase transmission the effluent water can be discharged from a single point only (near the utilization plant).
e. Fluids discharged from many holes may simply be merged together by joining wellhead branches to a single main pipeline (or more if required).
f. Aesthetic gains would result from the elimination of many elaborate wellhead equipment assemblies, and from the large reduction in the amount of escaping steam.

2.4.1 Flow regime of two-phase flow

A two-phase mixture can flow through a pipe in a variety of flow patterns as illustrated in Figure 4. The flow pattern determines the macroscopic behaviour of two-phase flow and is classified by visual observation. Classification can be useful since it affects parameters in different ways, such as pressure drop. One characteristic of horizontal flow in pipes is that a heavier phase (water) tends to be located close to the bottom due to gravity. In most cases, the gas phase pushes the liquid phase along the flow direction. Consideration of the flow regime in a two phase flow should be made; if the flow is slug flow, there can be problems with pipe support or ruptured pipes. Normally, the flow should be close to annular flow or stratified flow.

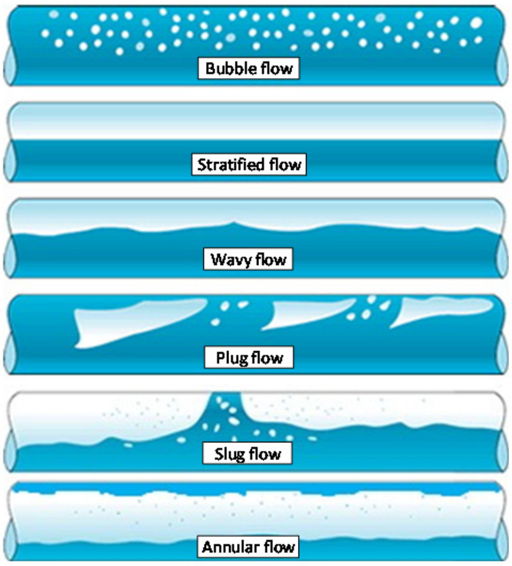

FIGURE 4: Two-phase flow regimes in horizontal pipes (www.globalspec.com)

Two-phase flow regimes are as follows (Pálsson, 2010):

Bubble flow: small bubbles are present in the flow and are dispersed everywhere in the pipe.
Stratified flow: the phases are completely separated with gas in the upper part and liquid in the lower part of the pipe.
Wavy flow: a stratified flow but with waves at the interface; appears at higher velocities.
Plug flow: bubbles join and form larger gas plugs; the plugs flow in the upper part of the pipe due to gravity.
Slug flow: waves in the flow reach the top of the pipe, closing the gas path in the top. Different momentum of the phases results in sudden pressure changes when the path closes. Shocks and vibrations are experienced in the flow which should be avoided if possible.
Annular flow: the liquid forms a film around the pipe walls. The gas core may contain liquid droplets. The film tends to be thicker at the bottom than at the top because of gravity.

These regimes depend on various conditions such as the transport properties of fluids (density difference, viscosity and surface tension), the mass and volume fraction in pipes, the velocity fraction between phases and geometry scales, and also pipe roughness. Flow regime maps can be used to determine the flow regime type with certain accuracy by using those parameters. Commonly used flow maps are (Pálsson, 2010):

a. Baker map, which is old and widely used;
b. Hoogendoorn map, which is considered to be more accurate than the Baker map;
c. Mandhane, Gregory, Aziz map, which is another old map which is considered better than the

two above;

d. The Mukherjee and Brill map, published in 1985;
e. The Spedding and Nguyen map, published in 1980; and
f. A universal flow regime map, which is relatively new (2003), published by Spedding et al.

The Baker map for horizontal two phase flow was published in 1955, and shows a plot of G/λ against $L\psi$, where G and L are the mass fluxes of the gas and liquid phase, respectively; and λ and ψ are calculated with the following formulas (Pálsson et al., 2006):

$$\psi = \left(\frac{0.0724}{\sigma_L}\right)\left(\frac{\mu_L}{0.0009}\left(\frac{1000}{\rho_L}\right)^2\right)^{1/3} \tag{13}$$

and

$$\lambda = \left(\frac{\rho_g}{1.2}\cdot\frac{\rho_L}{1000}\right)^{1/2} \tag{14}$$

where σ_L is the surface tension of the liquid.

The Baker map in Figure 5 indicates that the flow regime of two-phase flow of the Ulubelu geothermal pipelines is annular flow. The second map in the figure is the Mandhane, Gregory and Aziz map for horizontal flow (GPSA, 2004). This map also clearly predicts that annular flow is the flow regime for the Ulubelu geothermal pipeline.

As Pálsson (2010) says: All practical two-phase calculations are much more complex than single-phase calculations. It is very difficult to derive theoretical formulas for the properties that are involved in two-phase flow. In most cases, it is necessary to use experiments and measurements to develop empirical relationships.

In the two-phase flow pressure drop prediction by the separated flow model, the void fraction (α) is the most important fundamental parameter. It is the ratio of the steam flow cross-section to the total cross section:

$$\alpha = A_g / A \tag{15}$$

where A_g and A are the area of steam and the total area, respectively.

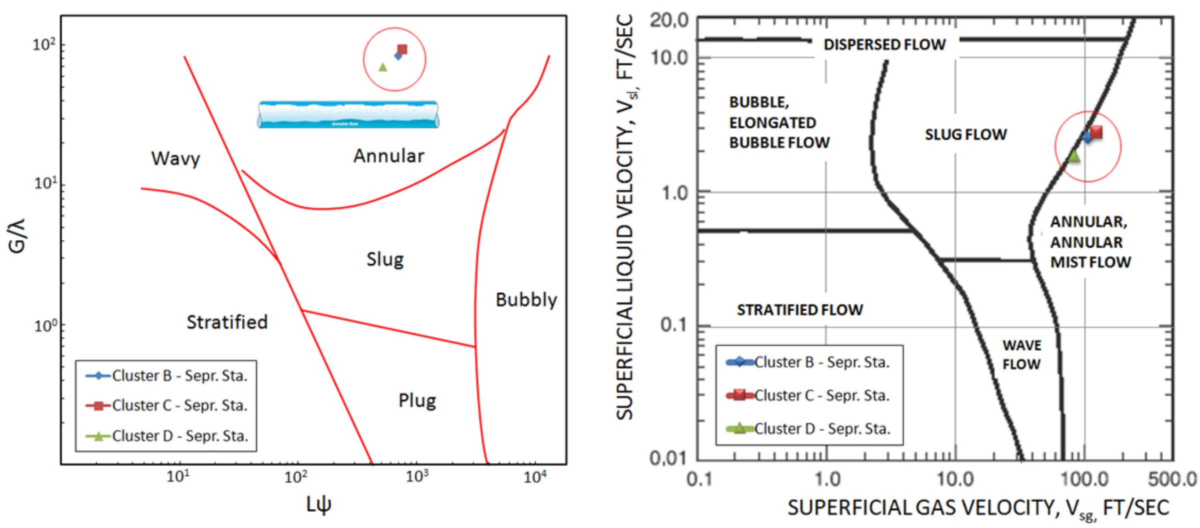

FIGURE 5: Horizontal flow regimes; Baker map on left and Mandhane et.al. map on right

2.4.2 Pressure drop due to length

A new void fraction correlation was proposed by Zhao et al. (2000). The new correlation is derived from the analysis of two-phase flow velocity distribution using the Seventh Power Law:

$$\frac{1 - \alpha}{\alpha^{7/8}} = \left[\left(\frac{1}{x} - 1\right)\left(\frac{\rho_g}{\rho_f}\right)\left(\frac{\mu_f}{\mu_g}\right)\right]^{7/8} \tag{16}$$

where x is the steam quality, f indicates the water phase and g indicates the gas phase.

To predict the two-phase pressure drop, an equivalent pseudo single-phase flow having the same boundary layer velocity distribution is assumed. The average velocity of the equivalent single-phase flow is used to determine the wall friction factor and, hence, the two-phase pressure drop. This method gives very good agreement with experimental data. The average velocity of the equivalent single-phase flow is also a very good correlating parameter for the prediction of geothermal two-phase pressure drops in a horizontal straight pipe.

The void fraction determines other two-phase parameters such as the average liquid phase velocity ($\bar{V}_f$), and the mean density (ρ). These, in turn, determine the two-phase pressure drop. The average liquid phase velocity can be expressed as (Zhao et al., 2000):

$$\bar{V}_f = 1.1\,(1 - x)\,\frac{\dot{m}\,(1 - x)}{\rho_f\,(1 - \alpha)\,A} \tag{17}$$

where $1.1(1\text{-}x)$ = Correction factor, mainly for entrainment;
$\dot{m}$ = Total mass flow rate (kg/s);
ρ_f = Density of water (kg/m^3); and
A = Cross-sectional area of pipe.

At this stage, a correction factor is introduced to account for the entrainment effect and a simplification is made in deriving the void fraction correction. It can be explained as a fraction of $1.1(1\text{-}x)$ of the liquid phase being left in the liquid phase boundary layer. The other fraction is entrained inside the gaseous phase as water droplets. When the steam quality decreases, the gaseous phase can carry less liquid. This means a higher percentage of the liquid is left in the boundary layer. The choice of the factor is mainly to give a good result rather than to find a rigorous theoretical justification. The average velocity of the equivalent single-phase flow ($\bar{V}$) can be calculated by (Zhao et al., 2000):

$$\frac{\bar{V}_f}{\bar{V}} = \frac{\left(1 - \sqrt{\alpha}\right)^{8/7} .\ \left(1 + \frac{8}{7}\sqrt{\alpha}\right)}{(1 - \alpha)} \tag{18}$$

Based on the average velocity of the equivalent single-phase flow ($\bar{V}$) and the density of water, the Reynolds number (*Re*) and friction factor (f) can be calculated using Equations 6-8. Then pressure drop due to the length of the pipe (ΔP_L) can be calculated by (Zhao et al., 2000):

$$\Delta P_L = \frac{f\,\rho_f\,\bar{V}^2}{2\,D_{in}\,(1 - AC)}\,.L \tag{19}$$

where ΔP_L = Pressure drop due to length (Pa);
AC = Acceleration correction; and
L = Length of pipe (m).

The acceleration correction (AC) is calculated using the following formula (Zhao et al., 2000):

$$AC = \frac{\dot{m}_g^2}{\rho_g (P A^2 \alpha)} \tag{20}$$

where P = Pressure (Pa); and
A = Inner cross-section area (m^2).

2.4.3 Pressure drop through different installations

When two-phase fluid flows through an installation such as a bend, its flow pattern is disturbed. Because of the complexity of the flow, it is very difficult to model the two-phase flow through a bend to derive a correlation analytically, and to provide a systematic calculation method for pressure drop across a bend. Many proposed correlations for predicting pressure drops in bends are empirical. Chisholm's (1983) correlation is the most popular.

In order to calculate the pressure drop for installations including bends, connections, expansion units and valves, the first two-phase multipliers (φ^2_{BLO}) for each component should be calculated by (Chisholm, 1983):

$$\varphi^2{}_{BLO} = 1 + \left(\frac{\rho_f}{\rho_g} - 1\right)(B\,x\,(1 - x) + x^2) \tag{21}$$

and

$$B = 1 + \frac{2.2}{K_{BLO}\left(2 + \left(\frac{r}{D_{in}}\right)\right)} \tag{22}$$

where x = Quality of steam;
K_{BLO} = $1.6fh$;
h = Equal length; and
r = Bend radius (m).

The total pressure drop through different installations can be calculated by:

$$\Delta P_{fi} = \frac{f\,\rho_m \bar{V}^2}{2\,D_{in}}\left(\varphi^2{}_{BLO,b}\,n_b h_b D_{in} + \varphi^2{}_{BLO,c}\,n_c h_c D_{in} + \varphi^2{}_{BLO,u}\,n_u h_u D_{in} + \varphi^2{}_{BLO,v}\,n_v h_v D_{in}\right) \tag{23}$$

where ΔP_{fi} = Pressure drop for the whole installation (Pa);
ρ_m = Density of mixture of water and steam (kg/m^3);
$\varphi^2_{BLO,b}$ = Two-phase multiplier for bends;
$\varphi^2_{BLO,c}$ = Two-phase multiplier for connections;
$\varphi^2_{BLO,u}$ = Two-phase multiplier for expansion units; and
$\varphi^2_{BLO,v}$ = Two-phase multiplier for valves.

2.4.4 Total pressure drop of two-phase flow fluid transmission

The total pressure drop of two-phase fluid transmission (ΔP_t) is expressed as:

$$\Delta P_t = \Delta P_L + \Delta P_{fi} + \Delta P_H \tag{24}$$

2.4.5 Pressure drop in the separator

The common types of separators used in geothermal power plants are the cyclone separator and the horizontal separator. In cyclone separators, the two-phase fluid enters tangentially at a high velocity, rotates several times, and the separated steam leaves through a central pipe. Recommended inlet velocities should be in the range of 25-40 m/s, the higher the better, but may be limited by the occurrence of unacceptable pressure drop. The pressure drop is estimated in terms of velocity head as follows (Walas, 1990):

$$\Delta P_{sep} = 4\,\rho \frac{V^2}{2\,g} \tag{25}$$

2.5 Pipe wall thickness-pressure class calculation

According to ASME B31.1, the minimum wall thickness required for design pressure and for temperatures not exceeding the allowable stress values of the material used, including allowances for mechanical strength, shall meet the following condition:

$$t_n \geq\; t_m = \frac{P\,D_o}{2\,(S_h\,E + P\,y)} +\; A \tag{26}$$

where t_n = Nominal pipe thickness, commercial pipe thickness available (m);
t_m = Requisite pipe thickness (m);
P = Design pressure (Pa);
D_o = Outer diameter of pipe (m);
S_h = Allowable stress of material at design temperature/hot stress (Pa);
E = Weld joint efficiency factor = 1, as this project uses seamless pipe;
y = Temperature dependent coefficient;
= 0.4 for steel with T < 482°C (Table 104.1.2(A) ASME B31.1); and
A = Thickness variation because of milling and corrosion (m).

The design pressure shall not be less than the pressure inside the pipe at the most severe condition expected during service. Hence, the pressure drop during operations shall be neglected (zero) and the pressure gained due to elevation changes shall be added to its initial pressure as the design pressure.

2.6 Mechanical stress analysis of the pipelines

2.6.1 Loads affecting pipeline system

Loads affecting a pipeline system consist of mechanical loads, thermal loads due to restraints and temperature gradients, and load effects because of supports, anchors and terminal movement. Mechanical loads consist of sustained loads that will weigh on continuously during the operating life of the pipeline system such as the weight of the pipe, piping components, insulation and occasional loads such as dynamic effects (impact forces due to external or internal conditions, wind and seismic loading, vibration) and weight effects (weight of medium transported and snow or ice loads if any). Loads on the pipeline systems can be calculated using the following conditions and equations and (Jónsson, 2010):

a. Sustained load criteria

The following condition must be met:

$$\frac{P\,D_o}{4\,t_n} + (0.75\,i)\left(\frac{M_A}{Z}\right) \;\leq\; S_h \tag{27}$$

where

$$Z = \frac{\pi}{32}\left(\frac{{D_o}^4 - D_{in}^4}{D_o}\right) \tag{28}$$

and i = Stress intensity factor, where (0.75 i) ≥ 1.0;
M_A = Sustained bending moment (Nm); and
Z = Section modulus (m^3).

Vertical sustained load:
Vertical sustained loads (q_{sv}) include pipe weight, piping component weight and insulation weight that can be calculated by:

$$q_{sv} = q_p + q_e \tag{29}$$

$$q_p = \pi\, g\, \rho_s \left(\frac{{D_o}^2 - D_{in}^2}{4}\right) \tag{30}$$

$$q_e = \pi\, g\, \rho_e \left(\frac{{D_e}^2 - D_o^2}{4}\right) \tag{31}$$

where q_p = Pipe weight (N/m);
q_e = Insulation weight (N/m);
ρ_s = Density of steel (kg/m^3) = 7850 kg/m^3 for a carbon steel pipe;
ρ_e = Density of insulation (kg/m^3) = 220 kg/m^3 for calcium silicate; and
D_e = Diameter of insulation (m).

b. Occasional load criteria

When occasional loads act upon a pipeline, the following condition must be fulfilled:

$$\frac{P\, D_o}{4\, t_n} + (0.75\, i)\left(\frac{M_A}{Z}\right) + (0.75\, i)\left(\frac{M_B}{Z}\right) \le kS_h \tag{32}$$

where M_B = Dynamic bending moment (Nm);
k = 1.20 if load is less than 1% operational time;
= 1.15 if load is less than 10% operational time; and
= 1.00 else.

Vertical occasional loads:
Vertical occasional loads (q_{dv}) consist of transported medium weight, snow weight (if applicable) and seismic vertical loads that can be calculated by:

$$q_{dv} = q_v + q_s + q_{jv} \tag{33}$$

$$q_v = \pi\, g\, \rho_v \left(\frac{D_{in}^2}{4}\right) \tag{34}$$

$$q_s = 0.2\, S\, D_e \tag{35}$$

$$q_{jv} = 0.5\, e\, q_o \tag{36}$$

$$q_o = q_v + q_p + q_e \tag{37}$$

where q_v = Medium weight (N/m);
q_s = Snow weight (N/m);
q_{jv} = Seismic vertical load (N/m);

ρ_v	=	Density of medium (kg/m^3);
S	=	Snow factor (N/m^2); and
e	=	Seismic factor.

Horizontal occasional load:
Horizontal occasional load (q_{dh}) is the maximum value of wind or seismic load that can be calculated by:

$$q_{dh} = max\ [\ q_w\ ,\ q_{jh}\ ] \tag{38}$$

$$q_w = C\ p_w\ D_e \tag{39}$$

$$p_w = v^2 /\ 1.6 \tag{40}$$

$$q_{jh} = e\ q_o \tag{41}$$

where	q_w	=	Wind load (N/m);
	q_{jh}	=	Seismic horizontal load (N/m);
	p_w	=	Wind pressure (N/m^2);
	C	=	Form factor, C = 0.6 for pipe; and
	v	=	Maximum wind speed (m/s).

2.6.2 Bending moment

A pipeline system is assumed to consist of segments of simple beams between supports. Thus, the bending moment at each support can be calculated by (Jónsson, 2010):

$$M_A = q_{sv}\ L_s^2 \tag{42}$$

$$M_B = \left(\sqrt{q_{dv}^2 + q_{dh}^2}\right).\ \ (L_s^2\ /\ 8) \tag{43}$$

where M_A, M_B = Sustained bending moment and dynamic bending moment (Nm), respectively;
L_s = The length between the two supports (m).

2.6.3 Length between supports

Pipe support shall be located at that point where the support can sustain a portion of the weight of the piping system plus any superimposed vertical loads. Hence, from the available bending moments and all available pipe loads, using Equations 32, 42 and 43, the length between the two supports (L_s) shall fulfil the following condition (Jónsson, 2010):

$$L_s^2 \leq \frac{\left[\ kS_h - \dfrac{P\ D_o}{4\ t_n}\right]\left[\dfrac{\pi}{4}\left(D_o{}^4 - D_{in}^4\right)\right]}{\left[D_o\ (0.75\ i)\left\{(q_{sv}) + \left(\sqrt{q_{dv}^2 + q_{dh}^2}\right)\right\}\right]} \tag{44}$$

2.7 Thermal expansion of the pipelines

Most of the pipelines in a geothermal power plant carry hot fluids such as steam and brine, but are installed in the field at ambient temperature. As a pipe heats up to the fluid's temperature inside the pipe, it experiences thermal stress and expands proportionally to the temperature difference between the environmental temperature and the fluid temperature. The pipe expansion (ΔL) can be calculated by (Jónsson, 2010):

$$\Delta L = \alpha \, L \, \Delta T \tag{45}$$

where α = Coefficient of thermal expansion (1/°C);
L = Length of pipe between two fixed ends (m); and
ΔT = Temperature difference (°C).

Thus, the thermal strain (ε_x) can be calculated with the following equation:

$$\varepsilon_x = \frac{\Delta L}{L} = \alpha \, \Delta T \tag{46}$$

The thermal stress (σ_x) and load on anchors (F) can be calculated by:

$$\sigma_x = E \, \varepsilon_x \tag{47}$$

$$F = A \, \sigma_x \tag{48}$$

where E = Young's modulus of the pipe material (N/m^2); and
A = The cross-sectional area on which the stress acts.

2.7.1 Expansion loop

An expansion loop is used to handle the thermal expansion of the pipe. Loops provide the necessary leg of piping in a perpendicular direction to absorb the thermal expansion. Expansion loops prevent overstress or fatigue of the pipe and the pipe supports. They also prevent distortions of the connection with other equipment installed on the pipe. There are several common types of expansion loops that can be used, such as zigzag or change direction and U-shape expansion loops. The selection between those types depends on the size of the expansion loop, availability of area and the cost.

According to ASME B31.1, given that the piping system is of uniform size and has no more than two anchors and no intermediate restraints, then the expansion loop meets the following requirement with respect to thermal expansion:

$$\frac{D_o \, Y}{(L - U)^2} \leq 208.3 \tag{49}$$

where D_o = Outer diameter of pipe (mm);
Y = Resultant movement to be absorbed by the pipe loop (mm);
L = Developed length of line axis (m); and
U = Anchor distance (m).

a. Zigzag type expansion loop

The zigzag type expansion loop means that the thermal expansion is absorbed by changing the direction of the pipeline. Figure 6 shows the use of a zigzag expansion loop in the pipeline system. In many cases, this design of expansion loop is cheaper than the U-type expansion loop. The design of a zigzag type expansion loop, as given in Figure 7, can be determined by (Jónsson, 2010):

$$Y = \alpha \, \Delta T \sqrt{(L_{T1}^2 + L_{T2}^2)} \tag{50}$$

$$L = L_1 + L_2 \tag{51}$$

$$U = \sqrt{(L_1^2 + L_2^2)} \tag{52}$$

$$L_{ANC} = \sqrt{(L_{T1}^2 + L_{T2}^2)} \tag{53}$$

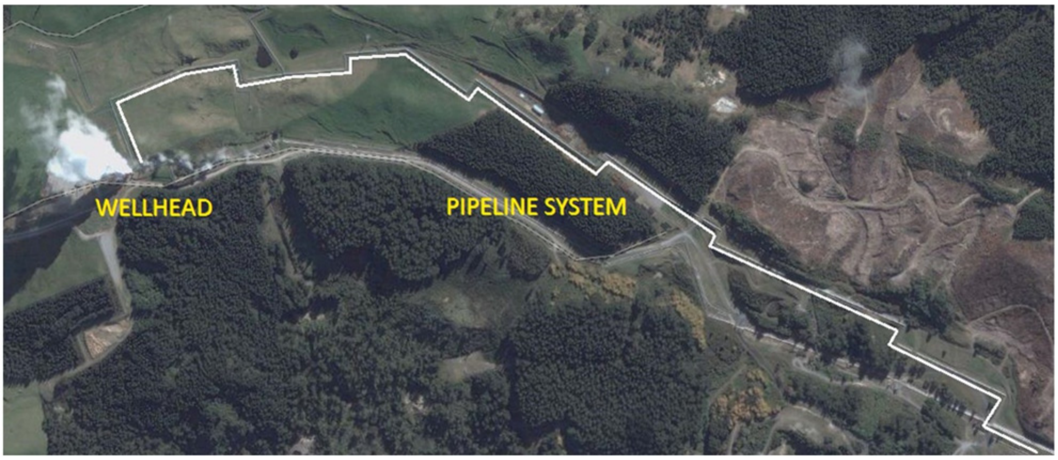

FIGURE 6: Satellite image of zigzag expansion loop at Wairakei geothermal field, New Zealand (Courtesy of Google Earth)

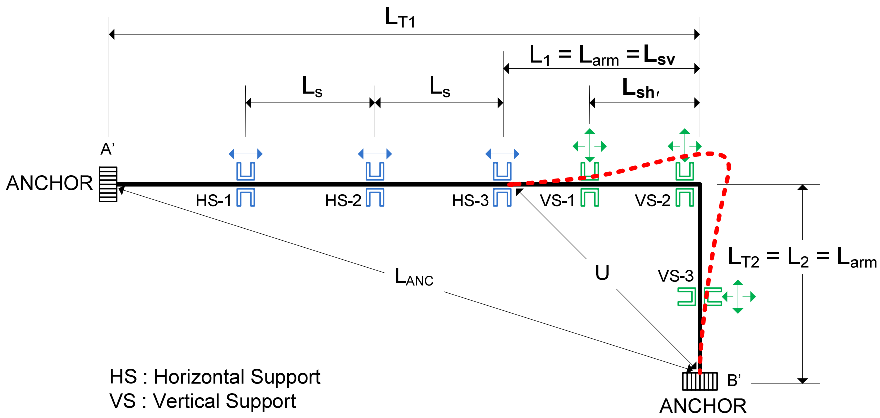

FIGURE 7: Expansion loop with change of direction (zigzag), red dotted line indicates the thermal deflection only, not the actual

Assume that $L_1 = L_2 = L_{arm}$ (Figure 7); Equations 49 to 53 can then be simplified to:

$$L_{arm} \geq \sqrt{\frac{D_o\ \alpha\ \Delta T\ L_{ANC}}{\left(208.3\ (\ 2 - \sqrt{2})^2\right)}} \tag{54}$$

where L_{T1}, L_{T2} = Length between anchors on each axis (m);
L_1, L_2, L_{arm} = Length of arm (m); and
L_{ANC} = Distance between two anchors (m).

b. U-shape expansion loop

U-shape expansion loops can be horizontal or vertical (Figure 8). A vertical loop is used to locate the loop at a road crossing. Vertical direction supports are provided to support the weight of the calculated span. Horizontal loops need a few more supports when compared with vertical loops in the bend length portion.

Figure 9 shows a diagram of a U-shape thermal expansion loop. There are some methods for estimating the loop's size. One method is the M.W. Kellogg method (British units). This method uses the Kellogg Chart (attached in Appendix II) to calculate the loop's size as follows (Kellogg, 1956):

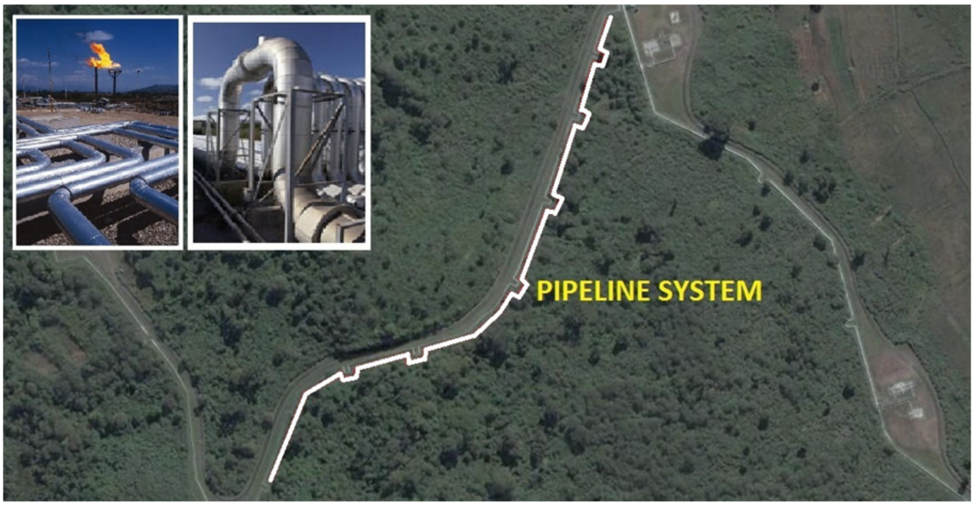

FIGURE 8: Satellite image of U-shape loop at Kamojang Indonesia and types of U-shape loops (horizontal and vertical) (Courtesy of Google Earth)

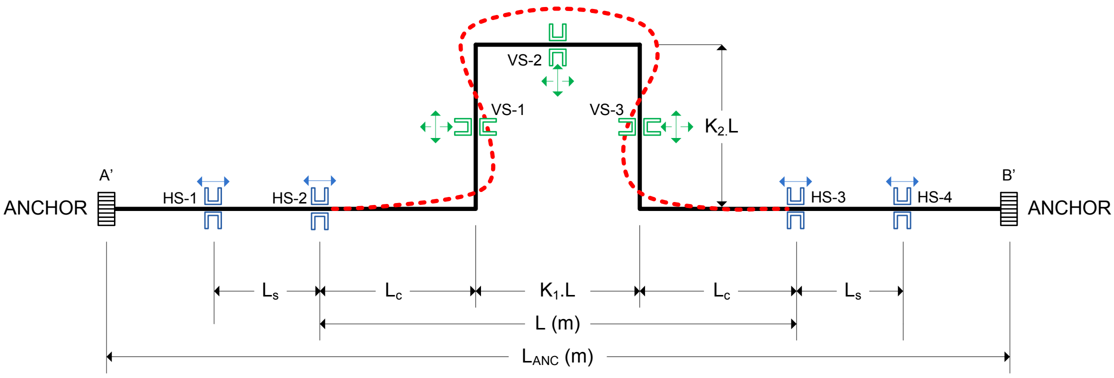

FIGURE 9: U-shape expansion loop, red dotted line indicates the thermal deflection only, not the actual

The y-coordinate of the chart is obtained by the following relationship:

$$y_{axis} = \frac{L^2\, S_A}{10^7\, D_o\, \Delta} \tag{55}$$

where L = Length between guide horizontal supports (ft);
S_A = Allowable stress range of material (psi); and
Δ = Expansion from A' to B' (inch).

The x-axis of the chart is K_2 and isolines for K_1 run across the chart. By selecting a value for either of the two parameters K_1 or K_2, the value of the other parameter is read from the chart and the dimensions of the loop are consequently obtained by multiplying L by the parameters as indicated in Figure 9. The distance from the guide horizontal supports to the loop (L_c) is found by the following formula (Figure 9):

$$L_c = \frac{1}{2}\, L\,(1 - K_1) \tag{56}$$

2.7.2 Length between horizontal and vertical supports

Pipe supports on expansion loops consist of two types. Horizontal supports allow the pipe to move axially (in the direction of the pipe) while vertical supports allow the pipe to move both axially and radially (in a direction perpendicular to the pipe) (Figure 10). The lengths between these two kinds of supports must be selected to meet the following condition (Jónsson, 2010):

$$\left(\frac{P\,D_o}{4\,t_n}\right)+\frac{(0.75\,i)\left\{(q_{sv}L_{sv}^2)+\left(\sqrt{(q_{dv}L_{sv}^2)^2+(q_{dh}L_{sh}^2)^2}\right)\right\}}{8\,Z}\leq\,kS_h \tag{57}$$

where L_{sv} = Length between vertical supports (m), equal to length of arm.;
L_{sh} =Length between horizontal supports (m)

FIGURE 10: From left to right, horizontal and vertical pipe supports
(pictures are taken from Nesjavellir Geothermal Power Station)

3. DESIGN AND RESULTS OF ULUBELU PROJECT PIPELINES

3.1 General overview

In order to select the optimum design and cost for a pipeline system, all possible design scenarios need to be considered and compared. For the Ulubelu geothermal project, 3 scenarios are calculated:

a. *Single-phase pipeline system*
   - Steam phase flow from each cluster to the interface point;
   - Individual separator at each cluster; and
   - Individual brine pipeline from each cluster to reinjection wells (clusters A and F).

b. *Two-phase pipeline system*
   - Steam and hot water in the same pipe from each cluster to a centralized separator station;
   - Separated steam transmitted from the centralized separator station to the interface point;
   - Centralized separator station located at cluster C; and
   - Brine pipeline from the centralized separator station to cluster A.

c. *Hybrid (combination) pipeline system*
   - Clusters B and C use two-phase pipeline system;
   - Cluster D uses single-phase pipeline system;

- Separator station at cluster C for two-phase flow (clusters B and C);
- Individual separator at cluster D for steam phase flow; and
- Brine pipelines from separator station at cluster C and separator at cluster D.

The access roads to each cluster have been built (see Section 1.2.1) and these will be used as pipe routes. It is the best option that can be selected, since the landscape and topography of these access roads is moderate and there are no high or low spots along the routes. Construction equipment will also have easy access in order to install the pipes.

3.2 Basic design data for calculations

3.2.1 General well data

Pressure drop in a pipeline is affected by elevation changes and the distance between the start and end points of a pipeline. These two parameters have significant effects on pipeline pressure drop. Tables 1 and 2 show the approximate elevation and distances of each cluster used in the calculations.

TABLE 1: Distances of each cluster

Cluster	**Approximate distance (m)**
A to C	1500
B to C	850
B to D	2270
D to F	2050
C to interface point	430
Interface point to A	1800

3.2.2 Environmental data

a. Temperature and humidity (Connusa, 2010)

i. Temperature
- Maximum temperature 24.6°C
- Minimum temperature 21.9°C
- Average temperature (annual) 22.8°C

ii. Relative Humidity
- Maximum relative humidity 89%
- Minimum relative humidity 77%
- Average relative humidity 84%

b. Wind (Connusa, 2010)

i. Maximum wind speed 8.3 km/hour
ii. Minimum wind speed 3.2 km/hour
iii. Average wind speed 3.4 km/hour
iv. Wind direction (dominant) Southwest

c. Seismicity

According to the latest edition of the Indonesian seismic design code SNI 03-1726-2002, Ulubelu geothermal field is located in seismic zone 5. Its coefficient of seismicity is 0.3 (maximum).

d. Barometric pressure

Ulubelu geothermal field is located at about 800 m a.s.l., hence the barometric pressure is assumed to be 920.84 mbar.

3.2.3 Interface point data (Connusa, 2010)

- Interface point location Within 25 m of power plant (Figure 2)
- Elevation at interface point 780 m
- Power capacity 2 x 55 MW – or 120 MW with 10% allowance
- Steam pressure 8.4 bar-a
- Steam dryness 99%

- Maximum steam flow rate — 8 ton/hour/MW, or 264 kg/s total steam
- Condensate temperature — 40°C
- Condensate pressure — 10 bar-a
- Condensate pH — 6-7 (neutral)

3.2.4 Well testing and results

All production wells have been drilled, and some of them have been tested, but the resulting data are limited due to inadequate production test facilities. Periodically, temperature and pressure logging are carried out for well monitoring. Wells UBL-02, 03, 05, 06, 07, and 08 have been discharge tested vertically and horizontally with limited separator sizes.

TABLE 2: Ulubelu's wells data

Type of well	Cluster	Elevation (m a.s.l.)	Well's name
Production wells	B	853	UBL-02 UBL-03 UBL-15
	C	770	UBL-05 UBL-06 UBL-07 UBL-08
	D	821	UBL-11 UBL-12 UBL-13 UBL-14
Reinjection wells	A	702	UBL-01 UBL-18
	F	688	UBL-17

a. Enthalpy

Enthalpy data were taken based on the temperature logging of each well, representing the estimated reservoir temperatures. The reservoir of Ulubelu's wells is a liquid-dominated system.

The reservoir temperatures can be figured out from the temperature profiles of the wells as seen in Figures 11 and 12. These temperature profiles were taken from the latest temperature logging and each well has a different heating time. Table 3 shows reservoir temperature and enthalpy of the liquid in the reservoir.

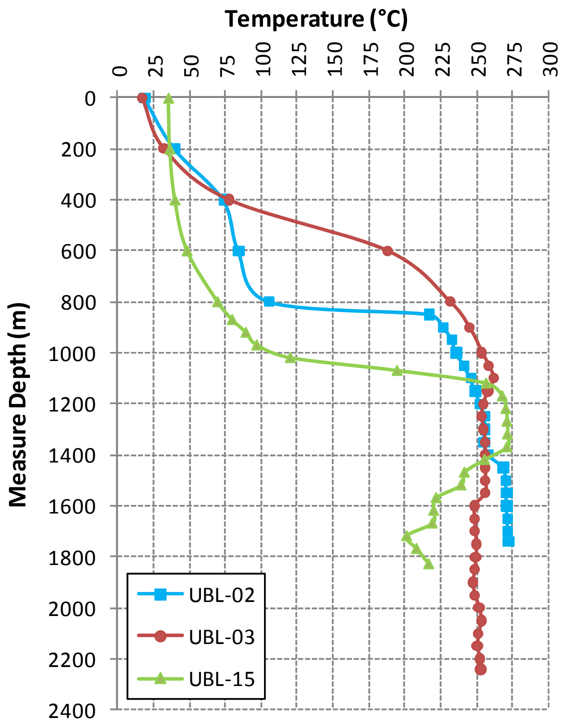

FIGURE 11: Temperature profiles of wells in cluster B

b. Wells production test data

Well production tests were carried out, giving limited data. These data do not represent the actual well conditions. Further tests should be carried out in order to determine the characteristic curves of the wells with greater accuracy. Four wells in cluster C (UBL-05 to UBL-08) have 0 bar-g shut-in wellhead pressure and about 20 bar-g maximum discharge pressure. These wells should be stimulated, by compressing the water level, in order to discharge the wells. Table 4 shows the production test results and Figure 13 shows the well production curves.

3.2.5 Pipe data

Specifications for the pipe used for this study are as follows:

- Pipe material — CS A106 Gr. B / A 53 Gr. B Seamless
- Young's modulus — 2 x 10^5 MPa
- Allowable stress at operating condition — 120 MPa

– Pipe roughness 0.045 mm
– Insulation material Calcium Silicate
– Corrosion allowance 3 mm

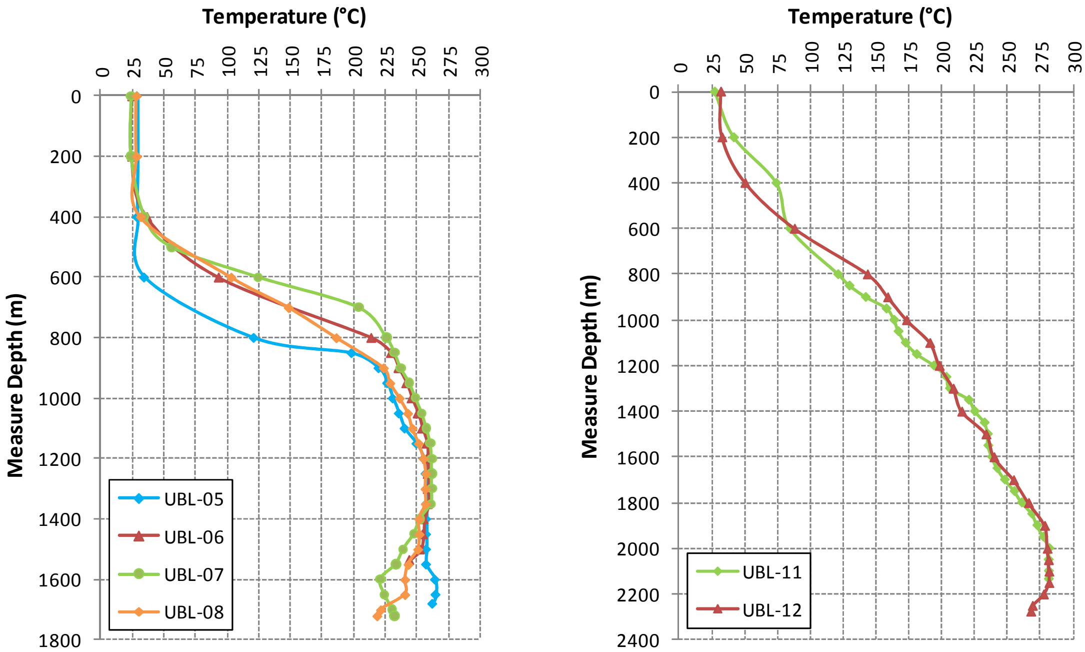

FIGURE 12: Temperature profiles of wells in cluster C on (left) and D (right)

TABLE 3: Enthalpy of production wells

Cluster	Well's name	Temp. (° C)	Enthalpy (kJ/kg)
B	UBL-02	271.13	1190.32
	UBL-03	251.89	1094.51
	UBL-15	270.15	1185.33
C	UBL-05	257.16	1120.34
	UBL-06	257.92	1124.09
	UBL-07	261.54	1142.03
	UBL-08	253.69	1103.3
D	UBL-11	281.64	1244.67
	UBL-12	280.57	1239.06
	UBL-13	No data available	
	UBL-14	No data available	

TABLE 4: Well production test data

Well's name	Well head pressure (bar-g)	Mass flow rate (ton/hour)	Well's name	Well head pressure (bar-g)	Mass flow rate (ton/hour)
UBL-02	15	154.20	UBL-05	14	502.00
UBL-02	20	141.18	UBL-05	15	469.90
UBL-02	24	141.70	UBL-05	17	360.00
UBL-03	15	220.43	UBL-08	13	363.60
UBL-03	20	212.10	UBL-08	17	222.20
UBL-03	34	140.75	UBL-08	18	180.38

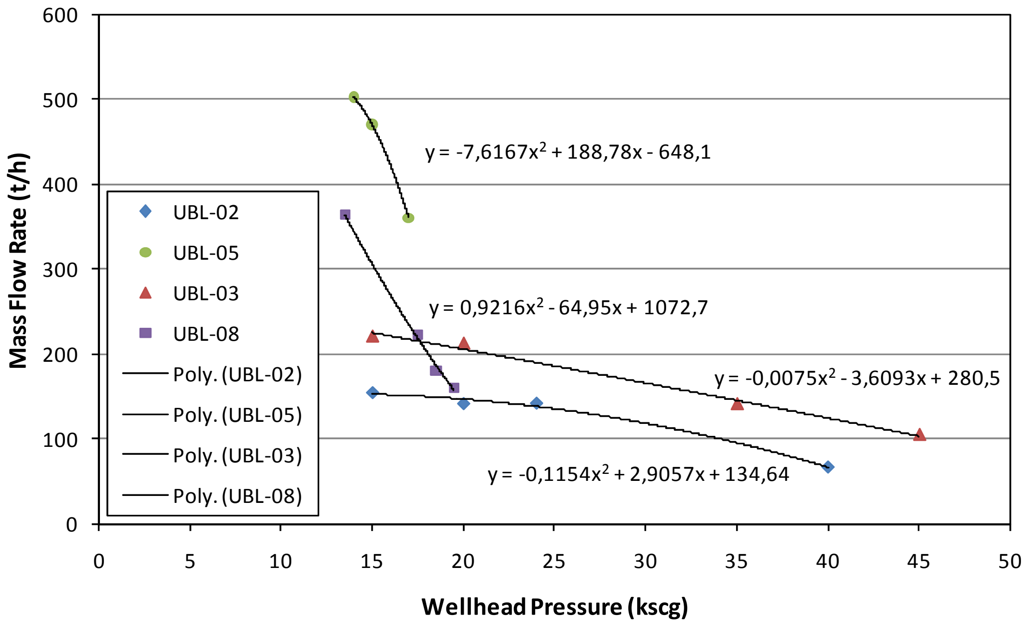

FIGURE 13: Well production curves

3.3 General assumptions

Some data required for the calculations were not available; hence, some assumptions were made in those cases. These assumptions are as follows:

a. Complete well discharge production test data were not available with reference to the trend of the preliminary well discharge test and pressure-temperature logging; it was assumed that cluster B supplied about 35% of the total flow required, cluster C supplied about 40% of the total flow required and cluster D supplied about 25% of the total flow required;
b. Enthalpy data were calculated by EES using the reservoir temperature obtained from temperature logging, as seen in Table 3; the well fluids were assumed to be liquid, with no steam phase in the wells;
c. A scrubber is installed close to the power plant past the interface point, hence there is no pressure drop caused by the scrubber;
d. The costs of materials (pipes, bends, connections and valves) were estimated from the cost of steel in USD per kg; the current price was found to be USD 0.788/kg (source : www.worldsteelprices.com);
e. Costs of separator, pipe supports and expansion loops were not included in the economic analysis;
f. Pipe insulation thickness was assumed to be 50 mm (Connusa, 2010);
g. Reinjection tests of 3 reinjection wells in cluster A and cluster F have not yet been completed. Wells were assumed to have sufficient capacity to receive brine and condensate from the systems;
h. Standard international (SI) units were used for the calculations.

3.4 Single-phase flow pipeline system calculations

This scenario is designed to transmit the steam phase flow from each cluster to the interface point located close to the power plant. Hence, a separator is located at each cluster close to the wellheads. Figure 14 shows a diagram of the pipelines and the mass balance of a single-phase flow pipeline system scenario. All calculations used equations presented in Section 2.

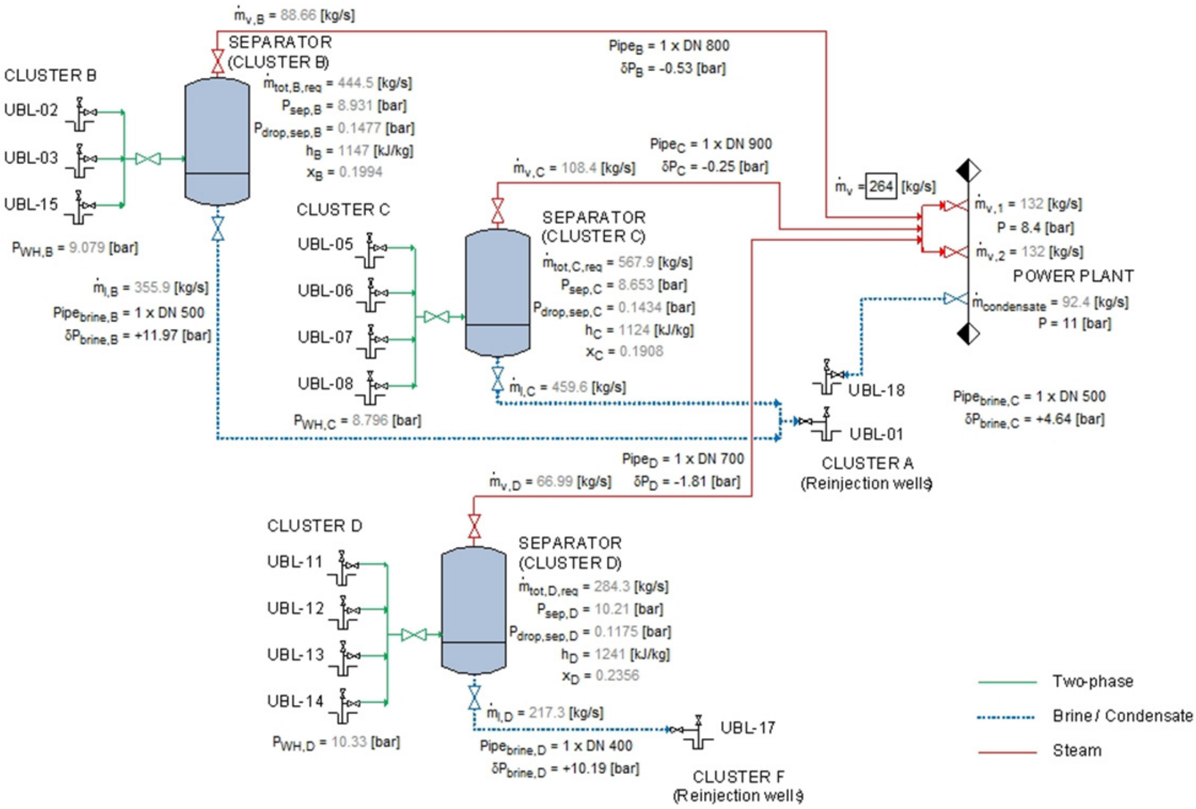

FIGURE 14: Diagram of single-phase flow pipeline scenario
(drawn and calculated with EES)

3.4.1 Pipeline design of cluster B – single-phase flow scenario

Data and results of the calculations for Cluster B pipelines are given in Tables 5 and 6, respectively. Based on the results provided in Table 6, the optimum design for a single-phase flow pipeline scenario for Cluster B is to use a single pipe for both steam and brine. Brine water is re-injected to cluster A. Expansion loop data indicated in Table 6 refer to Figures 7 and 9.

TABLE 5: Data for calculation of Cluster B pipeline - single-phase flow scenario

Data for pipeline calculation - Cluster B			
Steam pipeline		**Brine pipeline**	
Steam mass flow rate (kg/s)	88.66	Brine mass flow rate (kg/s)	355.9
Total enthalpy (kJ/kg)	2580	Total enthalpy (kJ/kg)	744
Length of pipe (m)	950	Length of pipe (m)	2350
Steam pipe elevation differences (m)	73	Brine pipe elevation differences (m)	151
Number of bends (units)	11	Number of bends (units)	28
Number of connections (units)	2	Number of connections (units)	2
Number of valves (units)	2	Number of valves (units)	2

3.4.2 Pipeline design of cluster C – single-phase flow scenario

Data and results of the calculations for Cluster C pipelines are given in Tables 7 and 8, respectively. Based on the calculations, the optimum design of a single-phase flow pipeline scenario for Cluster C is to use a single pipe for both steam and brine. Brine water is re-injected to cluster A.

TABLE 6: Calculation results for Cluster B pipelines - single-phase flow scenario

Cluster	**WHP (bar)**	**Scheme**	**NPD (mm)**	**Fluid**	**V (m/s)**	**P_sep (bar)**	**P_drop (bar)**	**P_int (bar)**	**Cost ($)**
B	9.07	1 pipe	800	steam	38.51	8.93	0.53	8.40	$133,000
		2 pipes	600	steam	34.18	8.97	0.57	8.40	$156,000
		1 pipe	500	brine	2.07	8.93	-11.97	20.90	$151,000
		2 pipes	300	brine	2.6	8.93	-9.98	18.91	$167,000

Pipe	**NPD**	**Thickness**	**Ls**	**U-shape loop (m)**					**Zigzag loop (m)**		
Fluid	**(mm)**	**(mm)**	**(m)**	**L_anc**	**L**	**Lc**	**K_1.L**	**K_2.L**	**Lsv**	**Lsh**	**L_anc**
steam	800	6.3	36	200	20	5	10	14	34	46	100
brine	500	6.3	18	200	20	5	10	13.6	10	35	80

WHP = well head pressure; NPD = nominal pipe diameter;
V = fluid velocity; P = pressure.
Subscripts sep, drop and int refer to separator, drop and interface point, respectively.

TABLE 7: Data for calculation of Cluster C pipeline - single-phase flow scenario

Data for pipeline calculation - Cluster C			
Steam pipeline		**Brine pipeline**	
Steam mass flow rate (kg/s)	108.4	Brine mass flow rate (kg/s)	459.6
Total enthalpy (kJ/kg)	2580	Total enthalpy (kJ/kg)	744
Length of pipe (m)	430	Length of pipe (m)	1500
Steam pipe elevation differences (m)	10	Brine pipe elevation differences (m)	68
Number of bends (units)	7	Number of bends (units)	17
Number of connections (units)	2	Number of connections (units)	2
Number of valves (units)	2	Number of valves (units)	2

TABLE 8: Calculation results of Cluster C pipelines - single-phase flow scenario

Cluster	**WHP (bar)**	**Scheme**	**NPD (mm)**	**Fluid**	**V (m/s)**	**P_sep (bar)**	**P_drop (bar)**	**P_int (bar)**	**Cost ($)**
C	8.79	1 pipe	900	steam	38.51	8.65	0.25	8.40	$91,000
		2 pipes	700	steam	31.83	8.62	0.22	8.40	$103,000
		1 pipe	500	brine	2.67	8.65	-4.64	13.30	$98,000
		2 pipes	400	brine	2.11	8.65	-4.90	13.55	$154,000

Pipe	**NPD**	**Thickness**	**Ls**	**U-shape loop (m)**					**Zigzag loop (m)**		
Fluid	**(mm)**	**(mm)**	**(m)**	**L_anc**	**L**	**Lc**	**K_1.L**	**K_2.L**	**Lsv**	**Lsh**	**L_anc**
steam	900	6.3	38	200	20	5	10	14	35	49	100
brine	500	6.3	18	200	20	5	10	13.6	10	35	80

3.4.3 Pipeline design of cluster D – single-phase flow scenario

Data and results of the calculations for Cluster D pipelines are given in Tables 9 and 10, respectively. Based on the calculations, the optimum design of a single-phase flow pipeline scenario for Cluster D is to use a single pipe for both steam and brine. Brine water is re-injected to cluster F.

TABLE 9: Data for calculation of Cluster D pipeline - single-phase flow scenario

Data for pipeline calculation - Cluster D			
Steam pipeline		**Brine pipeline**	
Steam mass flow rate (kg/s)	67	Brine mass flow rate (kg/s)	217.3
Total enthalpy (kJ/kg)	2580	Total enthalpy (kJ/kg)	744
Length of pipe (m)	3220	Length of pipe (m)	2050
Steam pipe elevation differences (m)	41	Brine pipe elevation differences (m)	133
Number of bends (units)	39	Number of bends (units)	23
Number of connections (units)	2	Number of connections (units)	2
Number of valves (units)	2	Number of valves (units)	2

TABLE 10: Calculation results of Cluster D pipelines - single-phase flow scenario

Cluster	**WHP (bar)**	**Scheme**	**NPD (mm)**	**Fluid**	**V (m/s)**	**P_sep (bar)**	**P_drop (bar)**	**P_int (bar)**	**Cost ($)**
D	10.33	1 pipe	700	steam	33.47	10.21	1.81	8.40	$330,000
		2 pipes	500	steam	31.36	10.81	2.41	8.40	$412,000
		1 pipe	400	brine	2.064	10.21	-10.19	20.40	$104,000
		2 pipes	250	brine	2.314	10.21	-8.86	19.07	$109,000

Pipe fluid	**NPD (mm)**	**Thickness (mm)**	**Ls (m)**	**U-shape loop (m)**					**Zigzag loop (m)**		
				L_anc	**L**	**Lc**	**K_1.L**	**K_2.L**	**Lsv**	**Lsh**	**L_anc**
steam	700	6.3	34	200	20	5	10	14	31	44	100
brine	400	7.1	18	200	20	5	10	13.6	12	33	80

3.4.4 Condensate pipeline from interface point to cluster A

The design of condensate pipelines is similar for all the scenarios, since the operating conditions are similar. Data and results of the calculations are given in Tables 11 and 12, respectively. Based on the calculations, the optimum design is to use double pipes.

TABLE 11: Data for calculation of condensate pipelines

Data of condensate pipeline calculation	
Condensate mass flow rate (kg/s)	92.4
Length of pipe (m)	1800
Condensate pipe elevation differences (m)	78
Number of bends (units)	21
Number of connections (units)	2
Number of valves (units)	2

TABLE 12: Calculation results of condensate pipelines

P_int (bar)	**Scheme**	**NPD (mm)**	**Fluid**	**V (m/s)**	**P_drop (bar)**	**P_o (bar)**	**Cost ($)**
11.00	1 pipe	250	water	1.927	-5.10	16.10	$48,000
	2 pipes	150	water	2.594	-1.50	12.50	$47,000

Pipe fluid	**NPD (mm)**	**Thickness (mm)**	**Ls (m)**	**U-shape loop (m)**					**Zigzag loop (m)**		
				L_anc	**L**	**Lc**	**K_1.L**	**K_2.L**	**Lsv**	**Lsh**	**L_anc**
water	2 x 150	4	12	200	12.5	5	2.5	1.875	12	16	500

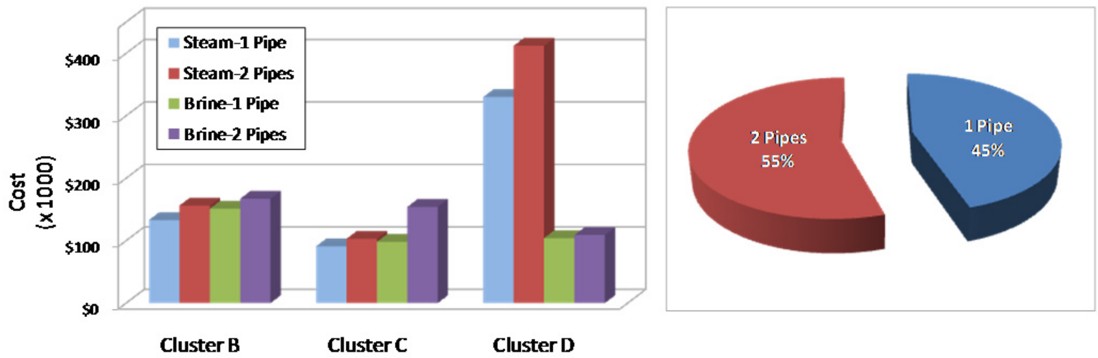

FIGURE 15: Charts comparing use of a single pipe or double pipes in a single-phase flow pipeline

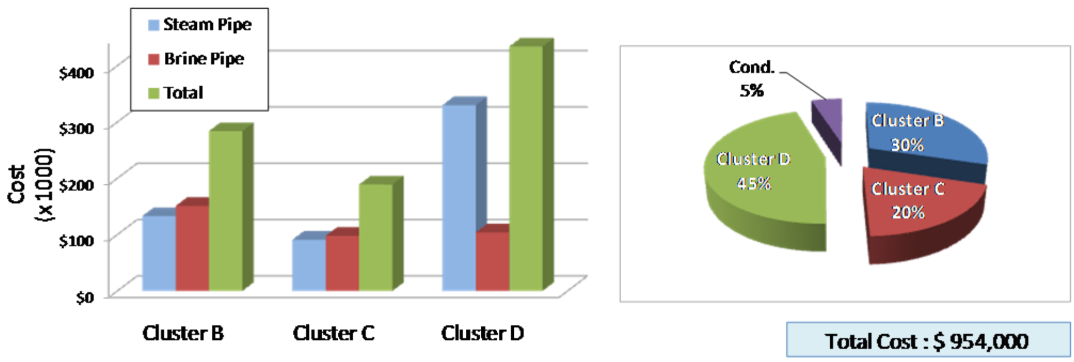

FIGURE 16: Charts showing total cost and percentage share for a single-phase flow pipeline

3.4.5 Comparison and total cost of single-phase flow pipeline scenario

Figure 15 shows a comparison between using a single pipe or parallel double pipes for the design of the single-phase flow pipeline scenario while Figure 16 shows total cost of the optimum design for a single-phase flow pipeline for each cluster, and the percentage share of each cluster in the cost. It is obvious that a single pipe design is more economical for a single-phase flow pipeline; the total pipeline cost equals about USD 954,000.

3.5 Two-phase flow pipeline system calculations

This scenario is designed to transmit two-phase flow from each cluster to the separator station located at cluster C, after which steam from the separator station is transmitted to the interface point close to the power plant. Figure 17 shows a diagram of the pipelines and the mass balance of a two-phase flow pipeline system scenario. All calculations used equations presented in Section 2.

3.5.1 Calculation results for a two-phase pipeline system

Calculations for a two-phase pipeline system were done for each cluster in the same way as for a single-phase pipeline. Complete data and results for each cluster are given in the tables attached in Appendix III; Table 13 gives a resume of the calculations for a two-phase pipeline system.

3.5.2 Comparison and total cost of two-phase flow pipeline scenario

Figure 18 gives a comparison of using single pipes or 2 parallel pipes for the design of a two-phase flow pipeline scenario. Figure 19 shows the percentages and total cost of the optimum design for a

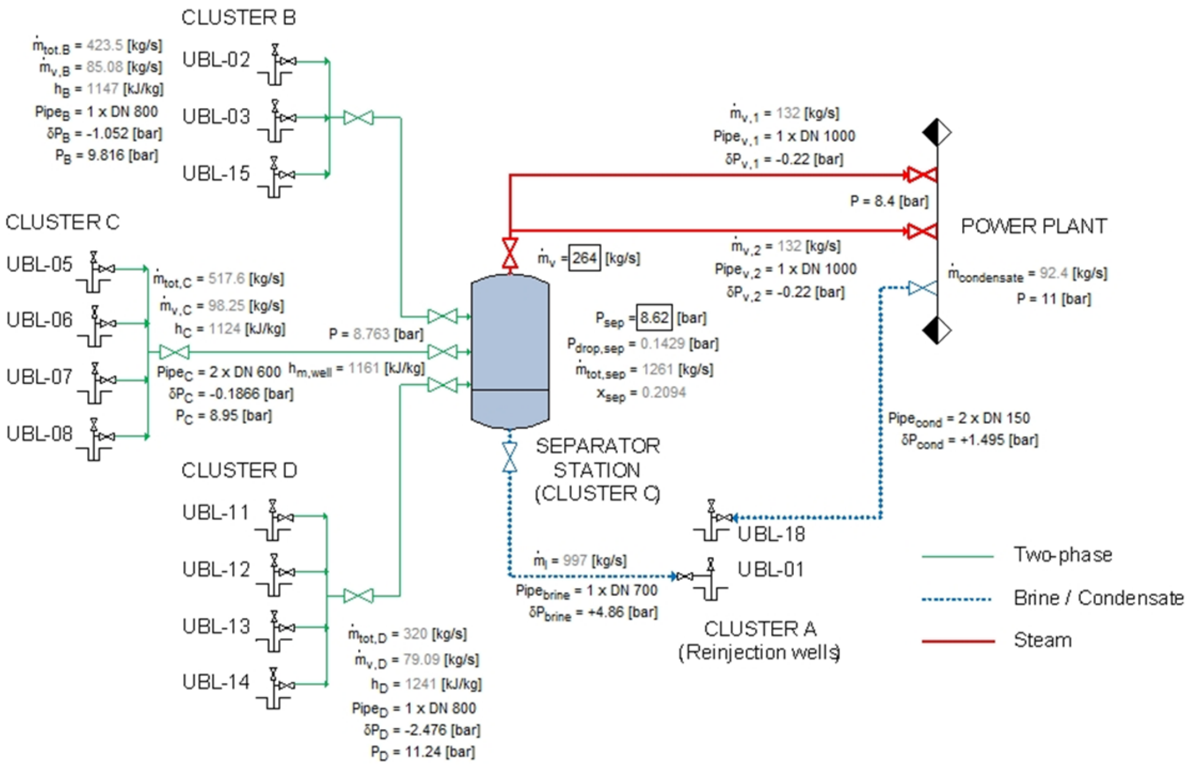

FIGURE 17: Diagram of two-phase flow pipeline scenario (drawn and calculated with EES)

two-phase flow pipeline. It is obvious that the single pipe design is more economical for a two-phase flow pipeline; the total pipeline cost is about USD 954,000.00.

TABLE 13: Calculation results of two-phase pipeline system

Pipeline	P_i (bar)	Scheme	NPD (mm)	Fluids	Flow rate (kg/s)	V (m/s)	P_drop (bar)	Cost ($)
Cluster B	9.82	1 pipe	800	two-phase	423.5	32.31	1.05	$120,000
Cluster C	8.95	2 pipes	600	two-phase	517.6	37.59	0.19	$14,000
Cluster D	11.24	1 pipe	800	two-phase	320	25.46	2.48	$412,000
Steam Sep.-Int.	8.62	2 pipes	1000	steam	264	37.95	0.22	$203,000
Brine	8.62	1 pipe	700	brine	997	2.92	-4.86	$158,000
Condensate	11.00	2 pipes	150	condensate	92.4	2.59	-1.50	$47,000
								$954,000

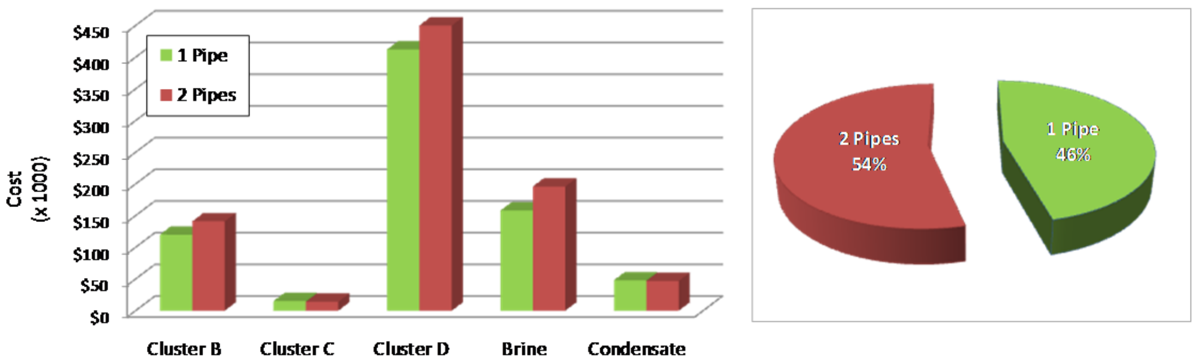

FIGURE 18: Charts comparing use of single pipe or double pipes in a two-phase flow pipeline

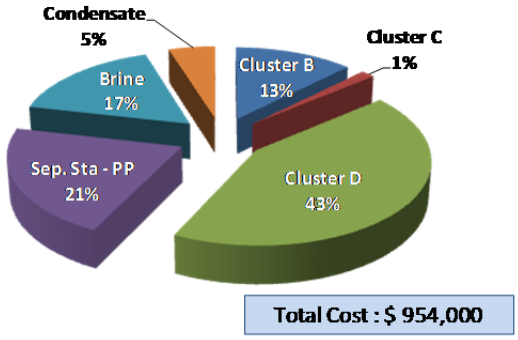

FIGURE 19: Percentages and total cost of a two-phase flow pipeline

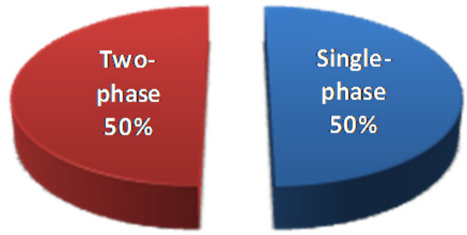

FIGURE 20: Cost comparison for the two pipeline scenarios, for single-phase flow and for two-phase flow

For a two-phase flow pipeline system, single pipe transmission is cheaper than double-pipe transmission, and cluster D has considerably higher costs than the others. Compared to a single-phase pipeline system, clusters B and C have significant cost reductions but, on the other hand, there is a significant cost for steam pipe transmission from the separator station at cluster C to the interface point of the power plant.

3.6 Analysis of single-phase and two-phase flow pipelines

With reference to the above calculations and from Figure 20, the total costs of the two scenarios for the Ulubelu Project gave similar results, about $954,000. In many cases, two-phase flow is more economical than single-phase flow. Table 14 and Figure 21 show a more detailed comparison between the scenarios and why these similar cost values occurred.

TABLE 14: Cost comparison of single-phase and two-phase flow (excluding condensate pipeline)

	Cost of pipe			Comparison of costs	
	Single-phase	**Two-phase**	**Δ Cost**	**Single-phase**	**Two-phase**
Cluster B	$284,000	$246,350	$37,650	53.55%	46.45%
Cluster C	$189,000	$158,400	$30,600	54.40%	45.60%
Cluster D	$434,000	$502,250	$68,250	46.36%	53.64%

Figure 21 shows that only in cluster D was the cost of two-phase flow higher than single-phase flow. It also shows that the sum of the cost differences in clusters B and C is nearly the same as the cost difference in cluster D. This is because when designing the single-phase flow in cluster D, brine water was re-injected to cluster F instead of cluster A as was done for two-phase flow. The distance from cluster D to cluster A is about 2500 m longer than to cluster F. It is very significant for the cost of the pipe. If the pipeline for cluster D was designed in the same manner as for clusters B and C, then the two-phase flow pipeline would be more economical than the pipeline for the single-phase flow, reducing the cost about $130,000.

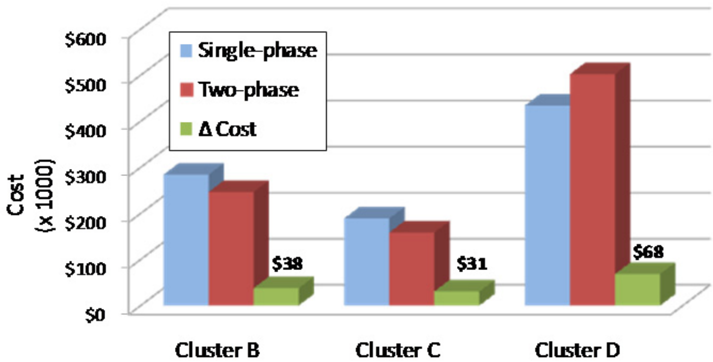

FIGURE 21: Cost comparison of single- and two-phase flow for each cluster

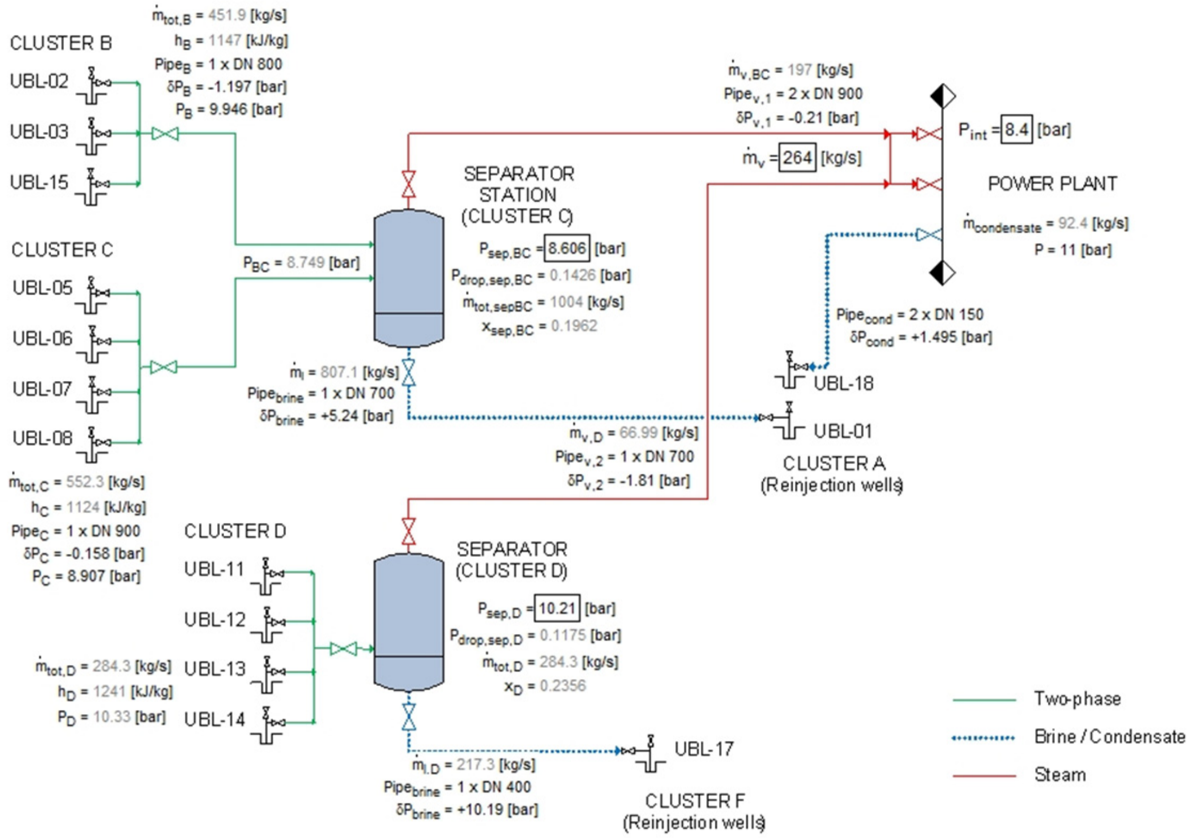

FIGURE 22: Diagram of hybrid flow pipeline scenario (drawn and calculated with EES)

3.7 Hybrid flow pipeline system calculations

Another pipeline design scenario can be introduced for the project. The most economic scenario possible should be a hybrid (combination) pipeline system, as shown in Figure 22. Clusters B and C are designed with a two-phase flow pipeline and cluster D is designed with a single-phase flow pipeline. A separator station for the two-phase flow from clusters B and C is located at cluster C and brine water is re-injected to cluster A. Cluster D has an individual separator at cluster D and steam is transmitted to the interface point while brine water is re-injected to cluster F. Figure 22 shows a diagram of the pipelines and the mass balance for the hybrid flow pipeline system scenario. All calculations were carried out in an identical manner to those for the single- and two-phase flow pipelines; the results are given in Table 15. Figure 23 shows the cost percentages for the hybrid pipeline system.

TABLE 15: Calculation results of a hybrid pipeline system

Pipeline	**P_i (bar)**	**Scheme**	**NPD (mm)**	**Fluid**	**Flow rate (kg/s)**	**V (m/s)**	**P_drop (bar)**	**Cost ($)**
Cluster B	9.95	1 pipe	800	two-phase	451.9	33.86	1.20	$120,000
Cluster C	8.91	1 pipe	900	two-phase	552.3	35.98	0.16	$15,000
Cluster D	10.33	1 pipe	700	steam	67	33.47	1.81	$330,000
Steam B&C	8.61	2 pipes	900	steam	197	35.17	0.21	$181,000
Brine B&C	8.61	1 pipe	700	brine	807.1	2.37	-5.24	$158,000
Brine D	10.21	1 pipe	400	brine	217.3	2.06	-10.19	$104,000
Condensate	11.00	2 pipes	150	condensate	92.4	2.59	-1.50	$47,000
								$955,000

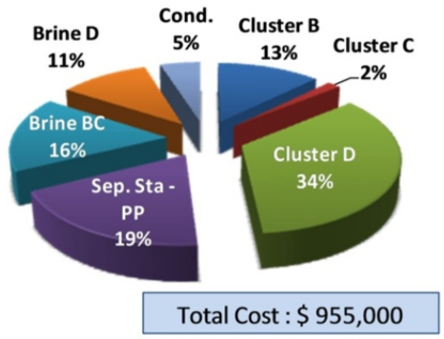

FIGURE 23: Percentages and total cost of hybrid pipeline system

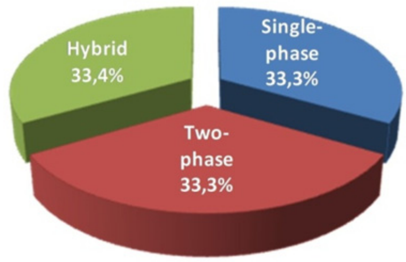

FIGURE 24: Cost comparison for the three pipeline scenarios, for single-phase flow, for two-phase flow and the hybrid system

The hybrid pipeline system scenario gives though a similar total cost as the single-phase flow and two-phase flow scenarios. Figure 24 shows the comparison. There were insignificant changes in the pipe diameter in the hybrid pipeline system.

3.8 Flow parameters

Based on the calculations of the 3 different scenarios, the flow parameters at each cluster should be set as given in Table 16. Wellhead pressure should be in the range of 8.8-11.3 bar at a given flow rate and enthalpy.

TABLE 16: Main flow parameters at each cluster in all scenarios

	Cluster B				Cluster C			
	P_drop (bar)	**WHP (bar)**	**Total flow rate (ton/hour)**	**Enthalpy (kJ/kg)**	**P_drop (bar)**	**WHP (bar)**	**Total flow rate (ton/hour)**	**Enthalpy (kJ/kg)**
Single-phase	0.5305	9.07	1600.2		0.2534	8.786	2044.44	
Two-phase	1.052	9.816	1524.6	1147	0.1866	8.95	1863.36	1124
Hybrid flow	1.197	9.95	1626.84		0.1579	8.91	1988.28	

	Cluster D			
	P_drop (bar)	**WHP (bar)**	**Total flow rate (ton/hour)**	**Enthalpy (kJ/kg)**
Single-phase	1.812	10.33	1023.48	
Two-phase	2.476	11.24	1152	1241
Hybrid flow	1.812	10.33	1023.48	

3.9 Final results for the Ulubelu pipelines

For the Ulubelu project, the results show that the hybrid pipeline system gives the optimum solution for transmitting well fluids to the power plant, but only at a small margin. Separated locations of reinjection wells lead to this scenario being a slightly better choice than the others, although the cost is similar. The hybrid system needs only 2 brine pipelines while the single-phase pipeline needs 3 brine pipelines; hence, the construction costs and costs for materials other than the pipeline are also higher. The two-phase flow pipeline needed an additional reinjection well to be drilled in cluster A since all brine and condensate would be re-injected into cluster A.

TABLE 17: Ulubelu project pipelines

Cluster	Scheme	Fluid	NPD (mm)	T (mm)	Ls (m)	U-shape loop (m)					Cost (x 1000)
						L_{anc}	L	L_c	K_1.L	K_2.L	
B - C	1 pipe	two-phase	800	7.1	36	200	20	5	10	14	$120
C - C	1 pipe	two-phase	900	7.1	38	200	20	5	10	14	$15
Sep sta. BC – Int.	2 pipes	steam	2 x 900	6.3	38	200	20	5	10	14	$181
Brine C - A	1 pipe	brine	700	6.3	19	200	20	5	10	14	$158
D - C	1 pipe	steam	700	6.3	34	200	20	5	10	14	$330
Brine D - F	1 pipe	brine	400	7.1	18	200	20	5	10	14	$104
Condensate - A	2 pipes	condensate	2 x 150	4	12	200	12.5	5	2.5	1.9	$47
											$955

A U-shape expansion loop is assumed to be the best way to handle thermal expansion in the pipelines since the pipe route was chosen to be alongside the existing access route and a zigzag expansion loop would need more land acquisition. The distances between the U-loops is 200 m and, referring to the calculations, would have the same design for all pipelines. Table 17 shows the final pipeline design of the Ulubelu geothermal project pipeline.

4. CONCLUSIONS AND DISCUSSION

In this report, calculations based on pipeline design modelling and thermodynamic analysis, were developed to optimize the pipeline design for a geothermal project. The results showed that the optimal design for the steam gathering system of the Ulubelu geothermal project should be a hybrid pipeline system, which is marginally better than the other two.

This report also confirms that the cost of a two-phase flow pipeline system is lower than for a single-phase flow pipeline system because both steam and water would be transmitted in the same pipe instead of through two individual pipes. On the other hand, this system is more complicated and rather unpredictable; hence, more attention should be paid when determining the design of the two-phase flow pipeline. Pressure drop is also higher in two-phase systems than when transmitting steam alone.

Site conditions such as environmental conditions, topography and pipeline layout greatly affect the selection of a pipeline system. Cluster D has the highest costs compared to the other clusters because it has the longest distance, whereas the mass flow rate is the lowest; hence, the pipeline route should be chosen to be as short as possible in order to minimize costs when designing the pipeline layout.

Calculations in this report were based on limited data; some approximations were made in order to get results. The calculations can be improved upon when more information and data become available. In some cases, such calculations are useful in the early parts of a project when data is still limited and the project needs to be immediately executed. These preliminary results can be used as a basis for a more detailed engineering design of steam gathering systems, so that a more accurate project design can be achieved, and such projects can be executed more efficiently in the future. This calculation model can also be used as a manual and design template for the selection and design of a pipeline system for other preliminary geothermal projects.

ACKNOWLEDGEMENTS

I would like to express my deepest gratitude to Dr. Ingvar B. Fridleifsson and Mr. Lúdvík S. Georgsson, for giving me the opportunity to attend the UNU Geothermal Training Programme in 2010 and also for their all their assistance. Many thanks also to all the staff of UNU GTP, Mr. Ingimar G. Haraldsson, Mrs. Dorthe H. Holm, Ms. Thórhildur Ísberg and Mr. Markús A.G. Wilde for their care and generous help. I am also sincerely grateful to my supervisors, Associate Professor Halldór Pálsson and Professor Magnus Th. Jónsson, both from the University of Iceland, for their help, guidance and advice during the project, and to Professor Páll Valdimarsson for his advice. I would also like to express my gratitude to the management of PT. Pertamina Geothermal Energy for permission to attend this programme. Finally, my deepest thanks go to my family, my dear wife Harinnita Maya Detta and my beloved son Marvello Andaru Aryasatya for their encouragement during these six months in Iceland.

REFERENCES

Armstead, H.C.H, 1983: *Geothermal energy*. E & FN Spon, Ltd., NY, USA, 389 pp.

Azimudin, T., 2008: Geothermal energy development in Indonesia, country update 2005-2008. In: Georgsson, L.S., Holm, D.H., and Fridleifsson, I.B. (eds.), *Papers presented at the 30th Anniversary Workshop of the United Nations University Geothermal Training Programme*. UNU-GTP, Reykjavík, CD, 8 pp.

Chisholm, D., 1983: *Two-phase flow in pipelines and heat exchangers*. Longman Higher Education, NY, USA, 324 pp.

Connusa, 2010: *FEED Ulubelu project unit 1 & 2*. PT. Pertamina Geothermal Energy, Indonesia, report.

GPSA, 2004: *Engineering data book*. Gas Processors Suppliers Association, USA, 821 pp.

Jónsson, M.Th., 2010: *Mechanical design of geothermal power plants.* UNU-GTP, Iceland, unpublished lecture notes.

Kellogg, M.W., 1956: *Design of piping systems* (rev. 2nd edition). John Wiley & Sons, Inc., NY, USA, 385 pp.

Pálsson, H., 2010: *Flow in pipelines*. UNU-GTP, Iceland, unpublished lecture notes.

Pálsson, H., Bergthórsson, E.S., and Pálsson, Ó.P., 2006: Estimation and validation of models two phase flow from geothermal wells. *10th International Symposium on District Heating and Cooling, Hanover University of Technology, Hanover, Germany*, 11 pp.

Walas, S.M., 1990: *Chemical process equipment, selection and design*. Butterworth-Heinemann, Washington, USA, 755 pp.

Waypanas PGE, 2008: *Drilling prognosis of Ulubelu Project*. PT. Pertamina Geothermal Energy, Indonesia, report.

Zhao, H.D., Lee, K.C., and Freeston, D.H., 2000: Geothermal two-phase flow in horizontal pipes. *Proceedings of the World Geothermal Congress 2000, Kyushu-Tohoku, Japan*, 3349-3353.

APPENDIX I: Example of EES calculations

```
"####################################################################################################"
"############ DESIGN OF TWO-PHASE FLOW PIPELINE SYSTEM - CLUSTER B TO CLUSTER C ( 1 PIPE ) ##############"
"####################################################################################################"
                                                                        "UNU-GTP 2010 - Novi Purwono"
PROCEDURE friction(Re,f_1,f_2:f)
    IF (Re<=2100) THEN
    f=f_1
    ELSE f=f_2
END

PROCEDURE Diameter(m_dot_v, rho_v:DIA)
i:=1
1: i:=i+1
F:=Lookup('Pipe Data', LookupRow('Pipe Data', 'Number', i), 'DN')
        D_o:=Lookup('Pipe Data', LookupRow('Pipe Data', 'DN', F), 'Do')                 "Pipe outside diameter, pipe table (mm)"
        thickness:=Lookup('Pipe Data', LookupRow('Pipe Data', 'DN', F), 'Thickness')    "Pipe thickness, pipe table (mm)"
        D_in:=(D_o-2*thickness)/1000                                                    "Pipe inside diameter (m)"
        A_pipe:=pi*(D_in/2)^2                                                           "Total area of pipe (m2)"
        V_sv:=(m_dot_v/rho_v)/A_pipe                                                    "SUPERFICIAL VAPOUR VELOCITY"
        If (V_sv>=40) Then GoTo 1
        DIA:=F
END

"########################################     MAIN PROGRAM     ##########################################"

">>>> DESIGN DATA <<<<"

m_dot_tot=423.5 [kg/s]
h=1147 [kJ/kg]
P=9.816 [bar]                          "Design pressure/Wellhead pressure (bar)"
H_s=853 [m]                            "Elevation of start point of pipeline system (m)"
H_e=770 [m]                            "Elevation of end point of pipeline system (m)"
g=9.81 [m2/s]                          "Gravity constant (m/s2)"

P_1=P*100000 [Pa]                      "Design pressure/Wellhead pressure at Pa"
rho_l=Density(Water,P=P,x=0)           "Density of liquid at design pressure (kg/m3)"
rho_v=Density(Water,P=P,x=1)           "Density of vapour at design pressure (kg/m3)"
x=Quality(Water,P=P,h=h)               "Steam quality"
rho_m=Density(Water,P=P,x=x)

mu_l=Viscosity(Water,P=P,x=0)          "Viscosity of liquid at design pressure (kg/ms)"
mu_v=Viscosity(Water,P=P,x=1)          "Viscosity of vapour at design pressure (kg/ms)"

m_dot_l=(1-x)*m_dot_tot                "Liquid mass flow rate (kg/s)"
m_dot_v=x*m_dot_tot                    "Vapour mass flow rate (kg/s)"

T=Temperature(Water,h=h,P=P)           "Operating temperature (C)"

">>>> Void Fraction (a) <<<<"

(1-a)/(a^(7/8))=(((1/x)-1)*(rho_v/rho_l)*(mu_l/mu_v))^(7/8)

">>>> Liquid phase velocity (V_bar_l) <<<<"

v_bar_l=1.1*(1-x)*((m_dot_tot*(1-x))/(rho_l*(1-a)*A_pipe))
```

```
">>>> Average velocity of equivalent single-phase velocity (V_bar) <<<<"

v_bar_l/v_bar=((1-sqrt(a))^(8/7)*(1+(8/7)*sqrt(a)))/(1-a)

">>>> Friction factor & Reynold Number <<<<"

Re=rho_l*v_bar*D_in/mu_l

f_1=64/Re
f_2=0.25/(log10((epsilon/1000/D_in)/3.7+5.74/Re^0.9))^2

CALL friction(Re,f_1,f_2:f)

">>>> Equivalent length <<<<"

h_b=20                                                  "equivalent length of bends"
h_c=20                                                  "equivalent length of connections, flow straight through"
h_u=20                                                  "equivalent length of expansion units"
h_v=13                                                  "equivalent length of valves"

L_p=850 [m]                                             "Pipe Length (m)"
n_b=CEIL((L_p/100)+2)                                   "number of bends"
n_c=2                                                   "number of connections"
n_u=0                                                   "number of expansion units"
n_v=2                                                   "number of valves"

">>>> Pressure drop due to length (P_drop_L) <<<<"

AC=m_dot_v^2/(rho_v*P_1*A_pipe^2*a)                     "Acceleration correction"
P_drop_L=(f*rho_l*v_bar^2/(2*D_in*(1-AC)))*L_p          " Unit in Pa"

">>>> Pressure drop through different installations <<<<"

r=Lookup('Pipe Data', LookupRow('Pipe Data', 'DN', DN), 'r')              "Bend radius"
h_eq=Lookup('Pipe Data', LookupRow('Pipe Data', 'DN', DN), 'h')           "Equivalent length"
K_BLOb=1.6*f*h_eq

Bb=1+2.2/(K_BLOb*(2+r/D_in))

Bc=1
Bu=1
Bv=1

Q2_BLOb=1+(rho_l/rho_v-1)*(Bb*x*(1-x)+x^2)              "The first two-phase multipliers for bends"
Q2_BLOc=1+(rho_l/rho_v-1)*(Bc*x*(1-x)+x^2)              "The first two-phase multipliers for connections"
Q2_BLOu=1+(rho_l/rho_v-1)*(Bu*x*(1-x)+x^2)              "The first two-phase multipliers for expansions"
Q2_BLOv=1+(rho_l/rho_v-1)*(Bv*x*(1-x)+x^2)              "The first two-phase multipliers for valves"

P_drop_fi=(f*rho_m*v_bar^2/(2*D_in))*(Q2_BLOb*n_b*h_b*D_in+Q2_BLOc*n_c*h_c*D_in+Q2_BLOv*n_v*h_v*D_in+Q2_BLOu*n_u
*h_u*D_in)

"CONTINUE ..............."
```

APPENDIX II: M.W. Kellogg U-shape expansion loop chart (Kellogg, 1956)

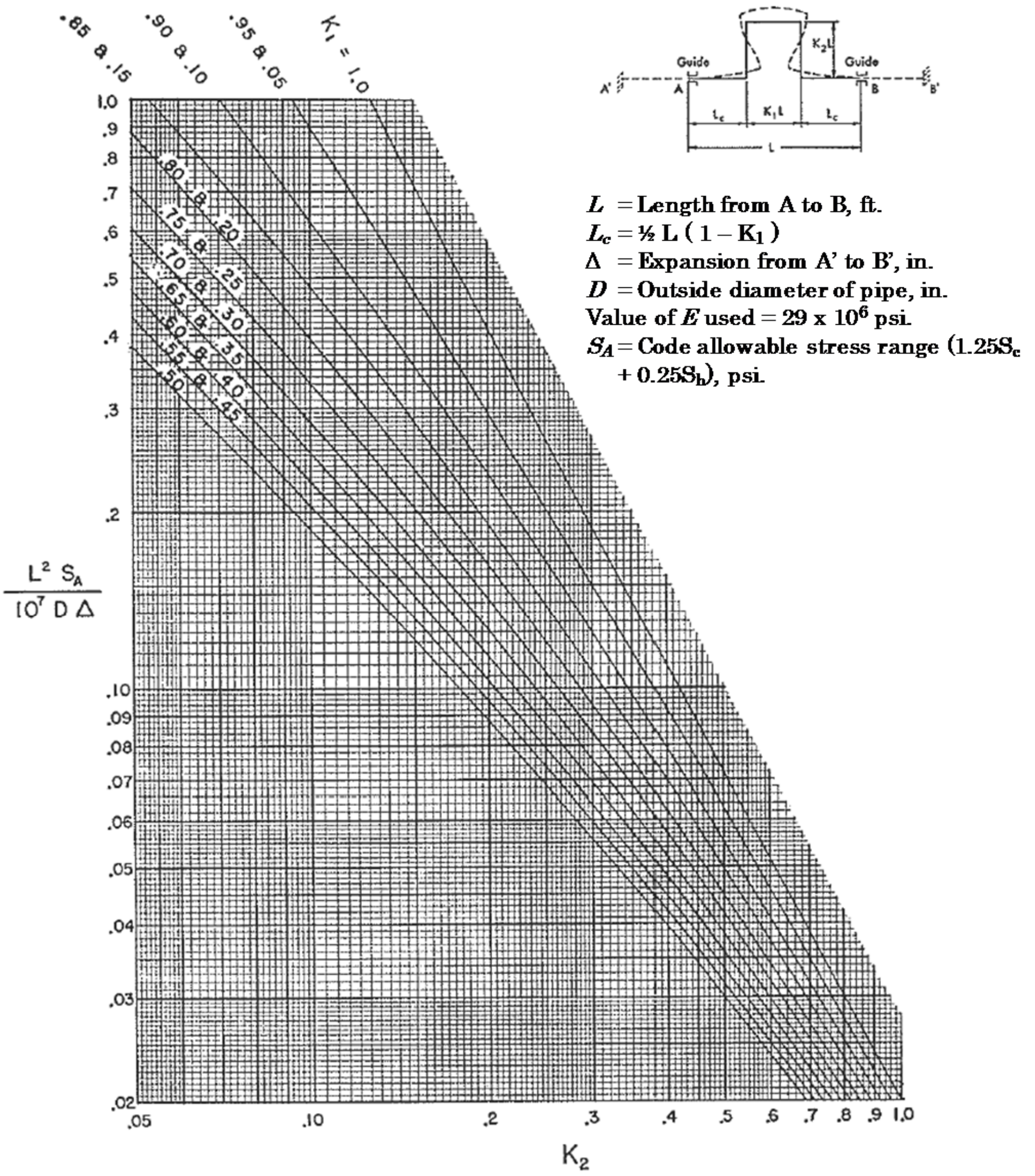

Multiply *L* by K_1 and K_2 to obtain dimensions of loop.

APPENDIX III: Calculation tables of two-phase flow pipeline

TABLE 1: Data for calculation of Cluster B pipeline - two-phase flow scenario

Data for pipeline calculation - Cluster B	
Two-phase mass flow rate (kg/s)	423.5
Total Enthalpy (kJ/kg)	1147
Length of pipe (m)	850
Two-phase pipe elevation differences (m)	83
Number of bends (units)	11
Number of connections (units)	2
Number of valves (units)	2

TABLE 2: Calculation results of Cluster B pipelines - two-phase flow scenario

Cluster	WHP (bar)	Scheme	NPD (mm)	Fluid	V (m/s)	P_drop (bar)	P_sep (bar)	Cost ($)
B	9.82	1 pipe	800	2-ph.	32.31	1.05	8.76	$120,000
		2 pipes	600	2-ph.	28.8	1.05	8.77	$141,000

Pipe fluid	NPD (mm)	Thickness (mm)	Ls (m)	U-shape loop (m)					Zigzag loop (m)		
				L_anc	L	Lc	K_1.L	K_2.L	Lsv	Lsh	L_anc
2-ph.	800	7.1	36	200	20	5	10	14	33	47	100

TABLE 3: Data for calculation of Cluster C pipeline - two-phase flow scenario

Data for pipeline calculation - Cluster C	
Two-phase mass flow rate (kg/s)	517.6
Total Enthalpy (kJ/kg)	1124
Length of pipe (m)	10
Two-phase pipe elevation differences (m)	0
Number of bends (units)	2
Number of connections (units)	2
Number of valves (units)	2

TABLE 4: Calculation results of Cluster C pipelines

Cluster	WHP (bar)	Scheme	NPD (mm)	Fluid	V (m/s)	P_drop (bar)	P_sep (bar)	Cost ($)
C	8.95	1 pipe	900	2-ph.	33.75	0.14	8.76	$15,000
		2 pipes	600	2-ph.	37.59	0.19	8.76	$14,000

Pipe fluid	NPD (mm)	Thickness (mm)	Ls (m)	U-shape loop (m)					Zigzag loop (m)		
				L_anc	L	Lc	K_1.L	K_2.L	Lsv	Lsh	L_anc
2-ph.	600	6.3	32	200	20	5	10	13.2	30	40	100

TABLE 5: Data for calculation of Cluster D pipeline - two-phase flow scenario

Data for pipeline calculation - Cluster D	
Two-phase mass flow rate (kg/s)	320
Total Enthalpy (kJ/kg)	1241
Length of pipe (m)	3120
Two-phase pipe elevation differences (m)	51
Number of bends (units)	39
Number of connections (units)	2
Number of valves (units)	2

TABLE 6: Calculation results of Cluster D pipelines - two-phase flow scenario

Cluster	WHP (bar)	Scheme	NPD (mm)	Fluid	V (m/s)	P_drop (bar)	P_sep (bar)	Cost ($)
D	11.24	1 pipe	800	2-ph.	25.46	2.48	8.76	$412,000
		2 pipes	600	2-ph.	22.66	2.48	8.76	$485,000

Pipe fluid	NPD (mm)	Thickness (mm)	Ls (m)	U-shape loop (m)					Zigzag loop (m)		
				L_anc	L	Lc	K_1.L	K_2.L	Lsv	Lsh	L_anc
2-ph.	800	7.1	36	200	20	5	10	14	32	48	100

TABLE 7: Data for calculation of steam pipeline - two-phase flow scenario

Data for steam pipeline calculation	
Steam mass flow rate (kg/s)	264
Separating pressure (bar)	8.62
Length of pipe (m)	430
Steam pipe elevation differences (m)	10
Number of bends (units)	6
Number of connections (units)	2
Number of valves (units)	2

TABLE 8: Calculation results of steam pipelines - two-phase flow scenario

Pipe	**Scheme**	**NPD (mm)**	**Fluid**	**V (m/s)**	**P_drop (bar)**	**P_int (bar)**	**Cost ($)**
Steam	2 pipes	1000	steam	37.95	0.22	8.40	$203,000

Pipe Fluid	**NPD (mm)**	**Thickness (mm)**	**Ls (m)**	**U-shape loop (m)**					**Zigzag loop (m)**		
				L_anc	**L**	**Lc**	**K_1.L**	**K_2.L**	**Lsv**	**Lsh**	**L_anc**
steam	1000	7.1	41	200	20	5	10	14	38	51	100

TABLE 9: Data for calculation of brine water pipeline - two-phase flow scenario

Data for brine water pipeline calculation	
Brine mass flow rate (kg/s)	997
Separating pressure (bar)	8.62
Length of pipe (m)	1500
Brine pipe elevation differences (m)	68
Number of bends (units)	17
Number of connections (units)	2
Number of valves (units)	2

TABLE 10: Calculation results of brine water pipeline - two-phase flow scenario

Pipe	**Scheme**	**NPD (mm)**	**Fluid**	**V (m/s)**	**P_drop (bar)**	**P_reinj (bar)**	**Cost ($)**
Brine	1 pipe	700	brine	2.92	-4.86	13.48	$158,000
	2 pipes	500	brine	2.89	-4.41	13.03	$196,000

Pipe fluid	**NPD (mm)**	**Thickness (mm)**	**Ls (m)**	**U-shape loop (m)**					**Zigzag loop (m)**		
				L_anc	**L**	**Lc**	**K_1.L**	**K_2.L**	**Lsv**	**Lsh**	**L_anc**
brine	700	7.1	20	200	20	5	10	14	2	40	75